NUREG-1824
Draft for Comment

EPRI 1011999
Preliminary Report

Verification and Validation of Selected Fire Models for Nuclear Power Plant Applications

Volume 7:
Experimental Uncertainty

January 2006

U.S. Nuclear Regulatory Commission
Office of Nuclear Regulatory Research
Washington, DC 20555-0001

Electric Power Research Institute
3412 Hillview Avenue
Palo Alto, CA 94303

Verification & Validation of Selected Fire Models for Nuclear Power Plant Applications

Volume 7: Experimental Uncertainty

NUREG-1824 **EPRI 1011999**

January 2006

U.S. Nuclear Regulatory Commission
Office of Nuclear Regulatory Research (RES)
Division of Risk Analysis and Applications
Two White Flint North, 11545 Rockville Pike
Rockville, MD 20852-2738

U.S. NRC-RES Project Manager
M. H. Salley

Electric Power Research Institute (EPRI)
3412 Hillview Avenue
Palo Alto, CA 94303

EPRI Project Manager
R. P. Kassawara

DISCLAIMER OF WARRANTIES AND LIMITATION OF LIABILITIES

THIS DOCUMENT WAS PREPARED BY THE ORGANIZATION(S) NAMED BELOW AS AN ACCOUNT OF WORK SPONSORED OR COSPONSORED BY THE ELECTRIC POWER RESEARCH INSTITUTE, INC. (EPRI). NEITHER EPRI NOR ANY MEMBER OF EPRI, ANY COSPONSOR, THE ORGANIZATION(S) BELOW, OR ANY PERSON ACTING ON BEHALF OF ANY OF THEM:

(A) MAKES ANY WARRANTY OR REPRESENTATION WHATSOEVER, EXPRESS OR IMPLIED, (I) WITH RESPECT TO THE USE OF ANY INFORMATION, APPARATUS, METHOD, PROCESS, OR SIMILAR ITEM DISCLOSED IN THIS DOCUMENT, INCLUDING MERCHANTABILITY AND FITNESS FOR A PARTICULAR PURPOSE, OR (II) THAT SUCH USE DOES NOT INFRINGE ON OR INTERFERE WITH PRIVATELY OWNED RIGHTS, INCLUDING ANY PARTY'S INTELLECTUAL PROPERTY, OR (III) THAT THIS DOCUMENT IS SUITABLE TO ANY PARTICULAR USER'S CIRCUMSTANCE; OR

(B) ASSUMES RESPONSIBILITY FOR ANY DAMAGES OR OTHER LIABILITY WHATSOEVER (INCLUDING ANY CONSEQUENTIAL DAMAGES, EVEN IF EPRI OR ANY EPRI REPRESENTATIVE HAS BEEN ADVISED OF THE POSSIBILITY OF SUCH DAMAGES) RESULTING FROM YOUR SELECTION OR USE OF THIS DOCUMENT OR ANY INFORMATION, APPARATUS, METHOD, PROCESS, OR SIMILAR ITEM DISCLOSED IN THIS DOCUMENT.

ORGANIZATION(S) THAT PREPARED THIS DOCUMENT:

U.S. Nuclear Regulatory Commission, Office of Nuclear Regulatory Research

Science Applications International Corporation

National Institute of Standards and Technology

ORDERING INFORMATION

Requests for copies of this report should be directed to EPRI Orders and Conferences, 1355 Willow Way, Suite 278, Concord, CA 94520, (800) 313-3774, press 2 or internally x5379, (925) 609-9169, (925) 609-1310 (fax).

Electric Power Research Institute and EPRI are registered service marks of the Electric Power Research Institute, Inc. EPRI. ELECTRIFY THE WORLD is a service mark of the Electric Power Research Institute, Inc.

COMMENTS ON DRAFT NUREG-1824 REPORT

This report is being published jointly by the U.S. Nuclear Regulatory Commission (NRC) and the Electric Power Research Institute (EPRI). Any interested party may submit comments on this report for consideration by the NRC and EPRI staffs. Comments may be accompanied by additional relevant information or supporting data. Please specify both the report number (Draft NUREG-1824) and the volume number in your comments, and send them by March 31, 2006, to the following address:

Chief Rules Review and Directives Branch
U.S. Nuclear Regulatory Commission
Mail Stop T-6D59
Washington, DC 20555-0001

For any questions about the material in this report, please contact:

Mark Henry Salley
Mail Stop T-10E50
U.S. Nuclear Regulatory Commission
Washington, DC 20555-0001
Phone: (301) 415-2840
Email: MXS3@nrc.gov

If EPRI members also wish to provide comments to EPRI, they may send them to the following address:

R.P. Kassawara
Electric Power Research Institute
3412 Hillview Avenue
Palo Alto, CA 94304
Phone: (650) 855-2775
Email: RKASSAWA@epri.com

CITATIONS

This report was prepared by

U.S. Nuclear Regulatory Commission,
Office of Nuclear Regulatory Research (RES)
Two White Flint North, 11545 Rockville Pike
Rockville, MD 20852-2738

Principal Investigators:
K. Hill
J. Dreisbach

Electric Power Research Institute (EPRI)
3412 Hillview Avenue
Palo Alto, CA 94303

Science Applications International Corp (SAIC)
4920 El Camino Real
Los Altos, CA 94022

Principal Investigators:
F. Joglar
B. Najafi

National Institute of Standards and Technology
Building Fire Research Laboratory (BFRL)
100 Bureau Drive, Stop 8600
Gaithersburg, MD 20899-8600

Principal Investigators:
K McGrattan
R. Peacock
A. Hamins

Volume 1, Main Report: B. Najafi, M.H. Salley, F. Joglar, J. Dreisbach
Volume 2, FDT^S: K. Hill, J. Dreisbach
Volume 3, FIVE-REV. 1: F. Joglar
Volume 4, CFAST: R. Peacock, J. Dreisbach, P. Reneke (NIST)
Volume 5, MAGIC: F. Joglar, B. Guatier (EdF), L. Gay (EdF), J. Texeraud (EdF)
Volume 6, FDS: K. McGrattan, J. Dreisbach
Volume 7, Experimental Uncertainty: A. Hamins

This report describes research sponsored jointly by U.S. Nuclear Regulatory Commission, Office of Nuclear Regulatory Research (RES) and Electric Power Research Institute (EPRI).

The report is a corporate document that should be cited in the literature in the following manner:

Verification and Validation of Selected Fire Models for Nuclear Power Plant Applications, Volume 7: Experimental Uncertainty, U.S. Nuclear Regulatory Commission, Office of Nuclear Regulatory Research (RES), Rockville, MD: 2005 and Electric Power Research Institute (EPRI), Palo Alto, CA. NUREG-1824 and EPRI 1011999.

ABSTRACT

There is a movement to introduce risk- and performance-based analyses into fire protection engineering practice, both domestically and worldwide. This movement exists in the general fire protection community, as well as the nuclear power plant (NPP) fire protection community.

In 2002, the National Fire Protection Association (NFPA) developed NFPA 805, *Performance-Based Standard for Fire Protection for Light-Water Reactor Electric Generating Plants, 2001 Edition.* In July 2004, the U.S. Nuclear Regulatory Commission (NRC) amended its fire protection requirements in Title 10, Section 50.48, of the *Code of Federal Regulations* (10 CFR 50.48) to permit existing reactor licensees to voluntarily adopt fire protection requirements contained in NFPA 805 as an alternative to the existing deterministic fire protection requirements. In addition, the nuclear fire protection community wants to use risk-informed, performance-based (RI/PB) approaches and insights to support fire protection decision-making in general.

One key tool needed to support RI/PB fire protection is the availability of verified and validated fire models that can reliably predict the consequences of fires. Section 2.4.1.2 of NFPA 805 requires that only fire models acceptable to the Authority Having Jurisdiction (AHJ) shall be used in fire modeling calculations. Further, Sections 2.4.1.2.2 and 2.4.1.2.3 of NFPA 805 state that fire models shall only be applied within the limitations of the given model, and shall be verified and validated.

This report is the first effort to document the verification and validation (V&V) of five fire models that are commonly used in NPP applications. The project was performed in accordance with the guidelines that the American Society for Testing and Materials (ASTM) set forth in *Standard E1355-04, "Evaluating the Predictive Capability of Deterministic Fire Models."* The results of this V&V are reported in the form of ranges of accuracies for the fire model predictions.

CONTENTS

FIGURES

TABLES

REPORT SUMMARY

This report documents the verification and validation (V&V) of five selected fire models commonly used in support of risk-informed and performance-based (RI/PB) fire protection at nuclear power plants (NPPs).

Background

Over the past decade, there has been a considerable movement in the nuclear power industry to transition from prescriptive rules and practices towards the use of risk information to supplement decision-making. In the area of fire protection, this movement is evidenced by numerous initiatives by the U.S. Nuclear Regulatory Commission (NRC) and the nuclear community worldwide. In 2001, the National Fire Protection Association (NFPA) completed the development of NFPA Standard 805, "Performance-Based Standard for Fire Protection for Light Water Reactor Electric Generating Plants 2001 Edition." Effective July, 16, 2004, the NRC amended its fire protection requirements in 10 CFR 50.48(c) to permit existing reactor licensees to voluntarily adopt fire protection requirements contained in NFPA 805 as an alternative to the existing deterministic fire protection requirements. RI/PB fire protection relies on fire modeling for determining the consequence of fires. NFPA 805 requires that the "fire models shall be verified and validated," and "only fire models that are acceptable to the Authority Having Jurisdiction (AHJ) shall be used in fire modeling calculations."

Objectives

The objective of this project is to examine the predictive capabilities of selected fire models. These models may be used to demonstrate compliance with the requirements of 10 CFR 50.48(c) and the referenced NFPA 805, or support other performance-based evaluations in NPP fire protection applications. In addition to NFPA 805 requiring that only verified and validated fire models acceptable to the AHJ be used, the standard also requires that fire models only be applied within their limitations. The V&V of specific models is important in establishing acceptable uses and limitations of fire models. Specific objectives of this project are:

Perform V&V study of selected fire models using a consistent methodology (ASTM E1355) and issue a report to be prepared by U.S. Nuclear Regulatory Commission Office of Nuclear Regulatory Research (RES) and Electric Power Research Institute (EPRI).

Investigate the specific fire modeling issues of interest to the NPP fire protection applications.

Quantify fire model predictive capabilities to the extent that can be supported by comparison with selected and available experimental data.

The following fire models were selected for this evaluation: (i) NRC's NUREG-1805 Fire Dynamics Tools (FDT^{S}), (ii) EPRI's Fire-Induced Vulnerability Evaluation Revision 1 (FIVE-

Rev. 1), (iii) National Institute of Standards and Technology's (NIST) Consolidated Model of Fire Growth and Smoke Transport (CFAST), (iv) Electricite de France's (EdF) MAGIC, and (v) NIST's Fire Dynamics Simulator (FDS).

Approach

This program is based on the guidelines of the ASTM E1355, "Evaluating the Predictive Capability of Deterministic Fire Models," for verification and validation of the selected fire models. The guide provides four areas of evaluation:

Defining the model and scenarios for which the evaluation is to be conducted,

Assessing the appropriateness of the theoretical basis and assumptions used in the model,

Assessing the mathematical and numerical robustness of the model, and

Validating a model by quantifying the accuracy of the model results in predicting the course of events for specific fire scenarios.

Traditionally, a V&V study reports the comparison of model results with experimental data, and therefore, the V&V of the fire model is for the specific fire scenarios of the test series. While V&V studies for the selected fire models exist, it is necessary to ensure that technical issues specific to the use of these fire models in NPP applications are investigated. The approach below was followed to fulfill this objective.

1. A set of fire scenarios were developed. These fire scenarios establish the "ranges of conditions" for which fire models will be applied in NPPs.
2. The next step summarizes the same attributes or "range of conditions" of the "fire scenarios" in test series available for fire model benchmarking and validation exercises.
3. Once the above two pieces of information were available, the validation test series, or tests within a series, that represent the "range of conditions" was mapped for the fire scenarios developed in Step 1. The range of uncertainties in the output variable of interest as predicted by the model for a specific "range of conditions" or "fire scenario" are calculated and reported.

The scope of this V&V study is limited to the capabilities of the selected fire models. There are potential fire scenarios in NPP fire modeling applications that do not fall within the capabilities of these fire models and therefore are not covered by this V&V study.

Results

The results of this study are presented in the form of relative differences between fire model predictions and experimental data for fire modeling attributes important to NPP fire modeling applications, e.g., plume temperature. The relative differences sometimes show agreement, but may also show both under-prediction and over-prediction. These relative differences are affected by the capabilities of the models, the availability of accurate applicable experimental data, and the experimental uncertainty of this data. The relative differences were used, in combination with some engineering judgment as to the appropriateness of the model and the agreement between model and experiment, to produce a graded characterization of the fire model's capability to predict attributes important to NPP fire modeling applications.

This report does not provide relative differences for all known fire scenarios in NPP applications. This incompleteness is due to a combination of model capability and lack of relevant experimental data. The first can be addressed by improving the fire models while the second needs more applicable fire experiments.

EPRI Perspective

The use of fire models to support fire protection decision-making requires that their limitations and confidence in their predictive capability is well understood. While this report makes considerable progress towards that goal, it also points to ranges of accuracies in the predictive capability of these fire models that could limit their use in fire modeling applications. Use of these fire models present challenges that should be addressed if the fire protection community is to realize the full benefit of fire modeling and performance-based fire protection. This requires both short term and long term solutions. In the short term a methodology will be to educate the users on how the results of this work may affect known applications of fire modeling. This may be accomplished through pilot application of the findings of this report and documentation of the insights as they may influence decision-making. Note that the intent is not to describe how a decision is to be made, but rather to offer insights as to where and how these results may, or may not be used as the technical basis for a decision. In the long term, additional work on improving the models and performing additional experiments should be considered.

Keywords

Fire	Fire Modeling	Verification and Validation (V&V)
Performance-based	Risk-informed regulation	Fire Hazard Analysis (FHA)
Fire safety	Fire protection	Nuclear Power Plant
Fire Probabilistic Risk Assessment (PRA)		Fire Probabilistic Safety Assessment (PSA)

PREFACE

This report is presented in seven volumes. Volume 1, the Main Report, provides general background information, programmatic and technical overviews, and project insights and conclusions. Volumes 2 through 6 provide detailed discussions of the verification and validation (V&V) of the following five fire models:

Volume 2 Fire Dynamics Tools (FDT^s)

Volume 3 Fire-Induced Vulnerability Evaluation, Revision 1 (FIVE-Rev1)

Volume 4 Consolidated Model of Fire Growth and Smoke Transport (CFAST)

Volume 5 MAGIC

Volume 6 Fire Dynamics Simulator (FDS)

Finally, Volume 7 quantifies the uncertainty of the experiments used in the V&V study of these five fire models.

FOREWORD

Fire modeling and fire dynamics calculations are used in a number of fire hazards analysis (FHA) studies and documents, including fire risk analysis (FRA) calculations; compliance with, and exemptions to the regulatory requirements for fire protection in 10 CFR Part 50; the Significance Determination Process (SDP) used in the inspection program conducted by the U.S. Nuclear Regulatory Commission (NRC); and, most recently, the risk-informed performance-based (RI/PB) voluntary fire protection licensing basis established under 10 CFR 50.48(c). The RI/PB method is based on the National Fire Protection Association (NFPA) Standard 805, "Performance-Based Standard for Fire Protection for Light-Water Reactor Generating Plants."

The seven volumes of this NUREG-series report provide technical documentation concerning the predictive capabilities of a specific set of fire dynamics calculation tools and fire models for the analysis of fire hazards in nuclear power plant (NPP) scenarios. Under a joint memorandum of understanding (MOU), the NRC Office of Nuclear Regulatory Research (RES) and the Electric Power Research Institute (EPRI) agreed to develop this technical document for NPP application of these fire modeling tools. The objectives of this agreement include creating a library of typical NPP fire scenarios and providing information on the ability of specific fire models to predict the consequences of those typical NPP fire scenarios. To meet these objectives, RES and EPRI initiated this collaborative project to provide an evaluation, in the form of verification and validation (V&V), for a set of five commonly available fire modeling tools.

The road map for this project was derived from NFPA 805 and the American Society for Testing and Materials (ASTM) Standard E1355-04, "Evaluating the Predictive Capability of Deterministic Fire Models." These industry standards form the methodology and process used to perform this study. Technical review of fire models is also necessary to ensure that those using the models can accurately assess the adequacy of the scientific and technical bases for the models, select models that are appropriate for a desired use, and understand the levels of confidence that can be attributed to the results predicted by the models. This work was performed using state-of-the-art fire dynamics calculation methods/models and the most applicable fire test data. Future improvements in the fire dynamics calculation methods/models and additional fire test data may impact the results presented in the seven volumes of this report.

This document does not constitute regulatory requirements, and RES participation in this study neither constitutes nor implies regulatory approval of applications based on the analysis contained in this text. The analyses documented in this report represent the combined efforts of individuals from RES and EPRI, both of which provided specialists in the use of fire models and other FHA tools. The results from this combined effort do not constitute either a regulatory position or regulatory guidance. Rather, these results are intended to provide technical analysis, and they may also help to identify areas where further research and analysis are needed.

Carl J. Paperiello, Director
Office of Nuclear Regulatory Research
U.S. Nuclear Regulatory Commission

ACKNOWLEDGMENTS

The work documented in this report benefited from contributions and considerable technical support from several organizations.

The verification and validation (V&V) studies for FDT^s (Volume 2), CFAST (Volume 4), and FDS (Volume 6) were conducted in collaboration with the U.S. Department of Commerce, National Institute of Standards and Technology (NIST), Building and Fire Research Laboratory (BFRL). Since the inception of this project in 1999, the NRC has collaborated with NIST through an interagency memorandum of understanding (MOU) and conducted research to provide the necessary technical data and tools to support the use of fire models in nuclear power plant fire hazard analysis (FHA).

We appreciate the efforts of Doug Carpenter and Rob Schmidt of Combustion Science Engineers, Inc. for their comments and contribution to Volume 2.

In addition, we acknowledge and appreciate the extensive contributions of Electricité de France (EdF) in preparing Volume 5 for MAGIC.

We also appreciate the efforts of organizations participating in the International Collaborative Fire Model Project (ICFMP) to Evaluate Fire Models for Nuclear Power Plant Applications, which provided experimental data, problem specifications, and insights and peer comment for the international fire model benchmarking and validation exercises, and jointly prepared the panel reports used and referred to in this study. We specifically appreciate the efforts of the Building Research Establishment (BRE) and the Nuclear Installations Inspectorate in the United Kingdom, which provided leadership for ICFMP Benchmark Exercise (BE) #2, as well as Gesellschaft fuer Anlagen-und Reaktorsicherheit (GRS) and Institut fuer Baustoffe, Massivbau und Brandschutz (iBMB) in Germany, which provided leadership and valuable experimental data for ICFMP BE #4 and BE #5. In particular, ICFMP BE #2 was led by Stewart Miles at BRE; ICFMP BE #4 was led by Walter Klein-Hessling and Marina Rowekamp at GRS, and R. Dobbernack and Olaf Riese at iBMB; and ICFMP BE #5 was led by Olaf Riese and D. Hosser at iBMB, and Marina Rowekamp at GRS. We acknowledge and sincerely appreciate all of their efforts.

We greatly appreciate Paula Garrity, Technical Editor for the Office of Nuclear Regulatory Research, and Linda Stevenson, agency Publication Specialist, for providing editorial and publishing support for this report. We also greatly appreciate Dariusz Szwarc, Nuclear Safety Professional Development Program participant, for his assistance finalizing this report.

LIST OF ACRONYMS

AGA	American Gas Association
AHJ	Authority Having Jurisdiction
ASME	American Society of Mechanical Engineers
ASTM	American Society for Testing and Materials
BE	Benchmark Exercise
BFRL	Building and Fire Research Laboratory
BRE	Building Research Establishment
CFAST	Consolidated Fire Growth and Smoke Transport Model
CFR	*Code of Federal Regulations*
EdF	Electricité de France
EPRI	Electric Power Research Institute
FDS	Fire Dynamics Simulator
FDT^s	Fire Dynamics Tools (NUREG-1805)
FHA	Fire Hazard Analysis
FIVE-Rev1	Fire-Induced Vulnerability Evaluation, Revision 1
FM-SNL	Factory Mutual & Sandia National Laboratories
FPA	Foote, Pagni, and Alvares
FRA	Fire Risk Analysis
GRS	Gesellschaft fuer Anlagen-und Reaktorsicherheit (Germany)
HRR	Heat Release Rate
IAFSS	International Association of Fire Safety Science
iBMB	Institut für Baustoffe, Massivbau und Brandschutz
ICFMP	International Collaborative Fire Model Project
IEEE	Institute of Electrical and Electronics Engineers
MCC	Motor Control Center
MQH	McCaffrey, Quintiere, and Harkleroad

MOU	Memorandum of Understanding
NBS	National Bureau of Standards (now NIST)
NFPA	National Fire Protection Association
NIST	National Institute of Standards and Technology
NPP	Nuclear Power Plant
NRC	U.S. Nuclear Regulatory Commission
NRR	Office of Nuclear Reactor Regulation (NRC)
RES	Office of Nuclear Regulatory Research (NRC)
RI/PB	Risk-Informed, Performance-Based
SDP	Significance Determination Process
SFPE	Society of Fire Protection Engineers
V&V	Verification & Validation

1
SELECTION OF DATA FOR MODEL EVALUATION

The methodology employed in this study follows the guidelines outlined in ASTM E 1355, *Standard Guide for Evaluating the Predictive Capability of Deterministic Fire Models* [Ref. 1]. One of the stated goals of such a study is to "Quantify the uncertainty and accuracy of the model results in predicting the course of events in similar fire scenarios." The subject of model accuracy is addressed in this volume through evaluation of the models. To accomplish the evaluation, the discussion in this volume focuses on experimental uncertainty.

The objective of this volume is not to provide a comprehensive description of the selected fire experiments. That information can be obtained in the original test reports, which are cited in the text. Rather, this volume serves as a link between the experiments and the models, especially with regard to experimental uncertainties, which are typically not reported. Also, certain parameters required as input by the fire models, like the radiation loss from the fire, are often not provided in the original test reports, because the information has not been measured. This document provides information that cannot be found in the original test reports for implementing the models and comparing the results to the experimental measurements.

1.1 Fire Experiments and Test Selection

This volume contains descriptions of the six sets of fire experiments that are being used in the evaluation of the five models considered in this report series. A number of the experiments were designed for the V&V studies, which were part of a series of Benchmark Exercises (BE) of the International Collaborative Fire Model Project (ICFMP) and a number were selected from the literature, based on the appropriateness of the data (FM/SNL, NBS).

In general, the experiments established steady fires burning in simple compartment geometries. The decision to include or exclude a particular test from a particular experimental test series as part of this validation study was made for a variety of reasons. Table 1-1 summarizes the experiments selected for the validation study in terms of the number of tests and the number of measurement types, as well as aspects of the fire and the compartment, including the fire heat release rate ($\dot{Q}$), and the compartment volume (V) and height (H).

Table 1-1: Overview of the Experiments Used for Model Evaluation

Series	Number of Tests	Number of Types of Measurements	$\dot{Q}$ (kW)	V (m^3)	H (m)
FM/SNL	3	4	500	1400	6.1
NBS	3	2	100	15	2.4
ICFMP BE #2	3	2	1800-3600	5900	19
ICFMP BE #3	15	8	400-2300	580	3.8
ICFMP BE #4	1	3	3500	74	5.7
ICFMP BE #5	1	4	400	73	5.6

The six fire experiments are introduced below, approximately in chronological order:

1. FM/SNL Test Series: 25 fire experiments conducted for the US NRC by Factory Mutual Research Corporation (FMRC) in 1985, under the direction of Sandia National Laboratories (SNL) [Ref. 2]. The primary purpose of these tests was to provide data with which to evaluate fire models used in hazard assessments of NPP enclosures. The results of three of these experiments have been used in the current validation study.

   The FM/SNL series involved a large number of measurements made during a long test series, but much of the data was never thoroughly analyzed. In particular, uncertainties were not provided. The three experiments selected were described in greater detail than the others, and these same three experiments have been used in a variety of prior validation studies. Estimates of uncertainty were determined from the test reports, the data itself, and supporting information, including conversations with one of the experimentalists.

2. NBS Multi-Compartment Test Series: 45 fire experiments, representing 9 different sets of test conditions, with multiple replicates of each set, that were conducted in a three-room suite at the National Bureau of Standards in 1985 (NBS, now the National Institute of Standards and Technology or NIST) [Ref. 3]. The primary purpose of these experiments was to evaluate fire models under development at the NBS at that time, in particular, the zone model CFAST. The results of three of these experiments have been used in the current validation study. Estimates of uncertainty were determined from the test reports, the data itself, and supporting information.

3. ICFMP Benchmark Exercise (BE) #2: A series of 8 fire experiments, representing 3 different sets of test conditions, that were conducted within a 19 m high test hall at VTT, the Finnish National Testing Laboratory during 1998 and 1999 [Ref. 4]. The test results were contributed to the International Collaborative Fire Model Project (ICFMP). All three cases, representing averaged results from the 8 tests, have been used in the current validation study.

4. ICFMP BE #3: A series of 15 fire experiments were conducted at NIST in 2003, which were partially funded by the U.S. NRC and NIST as part of the ICFMP. The results of all the experiments have been used in the current V&V study. All of the BE #3 experiments were

used. Re-analysis of the heat release rate data led to a revised report [Ref. 5], which included an expanded explanation of the heat release rate uncertainty estimate.

5. ICFMP BE #4: A series of small compartment kerosene pool fire experiments, conducted at the Institut für Baustoffe, Massivbau und Brandschutz (iBMB) of Braunschweig University of Technology in Germany in 2004 [Ref. 6]. The results of two of these experiments were contributed to the ICFMP, of which one has been used in the current V&V study. A malfunction in the measurement of the fuel mass loss rate was reported in Test 3, implying a level of uncertainty that is unacceptable for the current V&V study. The results from Test 1 were considered here.

6. ICFMP BE #5: A series of fire experiments in 2004 that involved realistically routed cable trays inside the same concrete enclosure at iBMB as BE #4 [Ref. 7]. The results of four tests were contributed to the ICFMP, of which one has been used in the current V&V study.

   BE #5 was conducted primarily for the evaluation of cable ignition and flame spread. The results were erratic, and no replicate experiments were performed. Given the primitive nature of the ignition and spread algorithms within the models, it was decided that only a qualitative analysis would be possible with the data from three of the four experiments. However, in one experiment, the first 20 min involved a fairly well-characterized ethanol pool fire burning on the opposite side of the compartment from the cable tray. This part of the experiment has been used as part of the model evaluation.

1.2 Measurement Selection

In addition to selecting individual experiments from the six test series, specific measurements were selected for use in the model evaluation. Section 2.4 of Volume 1 describes the rationale for the selection of these parameters, which was based on the need for fire safety in nuclear power plant applications. Because of the time and expense involved in conducting large-scale fire experiments, there is often a desire by the test laboratory to include as many measurements as possible. Unfortunately, much of the data goes unanalyzed, either because only a relatively small subset of the data is actually needed by the sponsoring organization, or because the budget for the project is exhausted in the preparation and execution of the experiments. In any event, there is a tremendous amount of fire test data that has never been thoroughly analyzed or used for V&V. Chapter 3 of this volume, which describes the experiments, provides some details about the decision to use, or exclude, a given measurement from the evaluation. This study evaluates the model calculations for the following 13 experimental parameters:

- Hot gas layer temperature
- Hot gas layer height
- Ceiling jet temperature
- Plume temperature
- Flame height
- Oxygen concentration
- Smoke concentration

- Compartment pressure
- Radiated heat flux to target
- Total heat flux to target
- Target temperature
- Total heat flux to walls
- Wall temperature

Table 1-2, taken from Table 2-3 of Volume 1 of this report, summarizes the measurements from each set of experiments that were used for comparison with the models. About 45 of the 78 (or 60 %) of the cells in Table 1-2 have entries that say, "no data," which means that either the measurement was not conducted, or that the data was flawed or otherwise suspect. Some of the tests provided more information than others, but none of the tests provided information for all of the parameters of interest. The graphical comparisons of measured and calculated results for each of the five fire models are presented in Appendix A of Volumes 2 through 6.

Table 1-2: Summary of the Test Series, Experiments, and Instrumentation Used for the Model Evaluation.

Fire Modeling Parameters	Selected Test Series/Experiments/Instrumentation					
	FM/SNL	NBS	ICFMP BE #2	ICFMP BE #3	ICFMP BE #4	ICFMP BE #5
	Tests 4,5, & 21	100A, 100O, 100Z	Part I, Cases 1, 2, 3	Tests 1-5, 7-10, 13-18	Test 1	Test 4
1. HGL temperature	Vertical arrays of thermocouples	Vertical arrays of thermocouples	Vertical arrays of thermocouples	Vertical arrays of thermocouples	Vertical arrays of thermocouples	Vertical arrays of thermocouples
2. HGL depth	Vertical arrays of thermocouples	Vertical arrays of thermocouples	Vertical arrays of thermocouples	Vertical arrays of thermocouples	Vertical arrays of thermocouples	Vertical arrays of thermocouples
3. Ceiling jet temperature	Thermocouple	No Data	No Data	Thermocouple	No Data	No Data
4. Plume temperature	Thermocouple	No Data	Thermocouple	No Data	No Data	No Data
5. Flame height	No Data	No Data	Photos	Photos	No Data	No Data
6. Gas concentrations	No Data	No Data	No Data	Oxygen meter	No Data	Oxygen meter
7. Smoke concentration	No Data	No Data	No Data	Laser transmission	No Data	No Data
8. Compartment pressure	No Data	No Data	No Data	Differential transducer	No Data	No Data
9. Radiant heat flux to target	No Data	No Data	No Data	Radiometers	No Data	No Data
10. Total heat flux to targets	No Data	No Data	No Data	Heat Flux Gauges	Heat Flux Gauges	Heat Flux Gauges
11. Target surface temperature	No Data	No Data	No Data	Thermocouples	Thermocouples	Thermocouples
12. Total heat flux to walls	No Data	No Data	No Data	Heat Flux Gauges	No Data	No Data
13. Wall surface temperature	No Data	No Data	No Data	Thermocouples	Thermocouples	Thermocouples

1.3 Fire Models

Section 2.2 of Volume 1 describes the selection of the five fire models considered in this study. These particular models were chosen based on the fact that most of them have been used fairly extensively to calculate fire conditions in NPP fire protection applications, or were developed by stakeholders within the nuclear industry for NPP fire protection applications. The models represent a wide range of capabilities and mathematical and computational sophistication. The models are:

- Two libraries of engineering calculations: FDTs and FIVE-Rev1
- Two two-zone models: CFAST and MAGIC
- One field model: FDS

Volumes 2 to 6 of this report describe these models in detail. Table 2-2 of Volume 1 lists the output provided by each of the fire models. While two of the models provide output for all of the 13 parameters listed above, the other three models considered in this study do not.

1.4 Uncertainty and Sensitivity

According to ASTM E1355 [Ref. 1], "Uncertainties in model inputs can lead to corresponding uncertainties in the model outputs. Sensitivity analysis is used to quantify these uncertainties in the model outputs based upon known or estimated uncertainties in model inputs." This section provides a discussion of the various forms of uncertainty that play a role in the model evaluation process. In the Appendices of Volumes 2 through 6, there are hundreds of graphs comparing time histories of experimental measurements and model predictions. Rarely do the curves lie exactly on top of each other, which raises the question as to how well did the models predict the experimental measurements. There are numerous methods of quantifying the "closeness" of the agreement. The degree to which the curves ought to match, however, depends on the application. In practice, each model user may have a different application. For example, knowing the gas temperature within a few degrees might be important if the application is detection, but an order of magnitude larger if the interest is the prediction of flashover. Fire protection engineers performing a hazard analysis are often content to demonstrate merely that the model is consistently "conservative"; that is, that a safety factor is implicit in the model formulation. Forensic experts, however, require the model to be as accurate as possible, with no built-in bias. In either case, model accuracy needs to be quantified. This means comparing model predictions to experimental measurements, as is done in the Appendices of Volumes 2 through 6, and then quantifying the differences between the two. The agreement between measurements and models is considered here in terms of the combined measurement and model input uncertainties.

1.4.1 Types of Uncertainty

The model evaluation process considers experimental uncertainty in two ways: (1) the sensitivity of the modeling results to uncertainty associated with input derived from experimental measurements, and (2) the uncertainty associated with the experimental measurement of the parameters of interest, that is, those parameters that are model output.

The former type of uncertainty is referred to here as *model input uncertainty*. This uncertainty does not represent model uncertainty in its totality. For example, the *intrinsic uncertainty* of a model is not accounted for by the *model input uncertainty*. That is, the physical and mathematical assumptions and methods that are an intrinsic part of the model formulation and its implementation are not part of the *model input uncertainty*. Examples of the *intrinsic model uncertainty* are the two-layer assumption in a zone fire model, the description of turbulence in a CFD fire model, or the grid size used in a CFD fire model. The *model input uncertainty* is related to the uncertainty of the input parameters to a model. Physical quantities like the thermal properties of the solid surfaces, chemical properties of the fuels, yields of the various products of combustion, and most importantly, the heat release rate of the fire, all have a certain degree of uncertainty. The uncertainty in the model output results are related to the uncertainty of each of the input parameters.

Beyond the input uncertainty, uncertainty associated with the experimental measurements is also considered in the model evaluation process. Measurements by thermocouples, heat flux gauges and gas analyzers all have a certain degree of uncertainty related to their operation, calibration, *etc*. This is referred to as *measurement uncertainty*. A measurement result is fully documented only when accompanied by a quantitative statement of its uncertainty. The uncertainty of experimental measurement results are typically broken into two types of uncertainty: instrument uncertainty and repeatability [Refs. 8, 9]. When the components of the measurement uncertainty are quantified, they are pooled into a combined uncertainty value that is a better representation of the total measurement uncertainty. The uncertainty is often expressed in terms of an expanded uncertainty, in which the confidence level that the measurement result falls within the expanded bounds is high. For an expansion factor of two, the uncertainty is related to two standard deviations ($2 \cdot \sigma$) and the confidence level corresponds to 95 %. Refs. [8, 9] discuss the various types of measurement uncertainty and ways to quantify them.

Typically, it is possible to provide rational estimates of the experimental *measurement uncertainty* and the experimental *model input uncertainty*. Both are related to measurements. The model *intrinsic uncertainty*, however, is far more difficult to quantify. *Intrinsic uncertainty* may have many components that may be coupled to each other. The interplay of various algorithms within a fire model, especially a CFD fire model, make it virtually impossible to dissect the various pieces, assess their uncertainty, and then combine the result into a single number. In this report, the fire model is used to simulate the experiments, and then the effects of *measurement uncertainty* and the model sensitivity to *model input uncertainty* are considered as possible sources of the difference between the model calculation results and the measurements.

As an example, Figure 1-1 shows the measured and the simulated temperature as a function of time for a hypothetical scenario. For simplicity, measurements and model results are compared at the time of their respective maximum values in this report. In the case shown in Figure 1, the maxima occur nearly 600 s after ignition, albeit at somewhat different times. The uncertainty bars in Figure 1-1 do not overlap near 600 s, and there are significant differences between the peak value (M_p) of the model prediction and the peak value of the experimental measurement (E_p). The *measurement uncertainty* and the sensitivity to *model input uncertainty* are also shown in Figure 1-1 as a function of time, and are represented as a set of circles. The purpose of this volume is to determine how much of the relative difference between the models and measurements can be attributed to a combination of the measurement and model input uncertainties.

1.4.2 Methodology for Evaluating the Models

The process of deducing the predictive capability of the model from the quantitative results is documented in Volumes 1 to 6 of this report series. Appendix A in each volume contains detailed comparisons of model predictions and experimental measurements. Two criteria are used to characterize the predictive capability of the fire models. The criteria are described in Section 2.6.2 of Volume 1. Chapter 6 in Volumes 2 to 6 describes how the quantitative results were used to arrive at the characterization of predictive capability for each of the models under consideration.

In the approach used in Volumes 2 to 6 of this report, model predictions and measurements are compared in terms of the relative difference between their maximum values:

$$\varepsilon = \frac{\Delta M - \Delta E}{\Delta E} = \frac{\left(M_p - M_o\right) - \left(E_p - E_o\right)}{\left(E_p - E_o\right)} \tag{1.1}$$

where ΔM is the difference between the peak value of the model prediction (M_p) and its baseline value (M_o), and ΔE is the difference between the peak value of the experimental measurement (E_p) and its baseline value (E_o). The parameter ε represents the relative difference between model predictions and measurements. In this study, the significance of the value of ε is considered through comparison with the combined relative expanded (2σ) uncertainty of ε, denoted as U_ε. The measurement and model results and their uncertainties are graphically represented in Fig. 1-1. The values of ΔM and ΔE in Fig. 1-1 are about 220 ^{o}C and 280 ^{o}C, respectively, while the relative expanded measurement and model input uncertainties, U_e and U_m, are about ±10 % and ±20 %, about the respective peaks.

Propagation of error for ε in Eq. 1.1 leads to an expression for the absolute combined expanded (2σ) uncertainty [Ref. 8], which is given by:

$$U_\varepsilon = (\varepsilon + 1)\,(\,U_e^{\,2} + U_m^{\,2}\,)^{\,½} \tag{1.2}$$

where U_e is the relative expanded (2σ) measurement uncertainty and U_m is the relative expanded (2σ) model input uncertainty. This formulation considers the functional form of Eq. 1.1. Because ε is typically small, the term $(\varepsilon + 1)$ is approximately one, so that:

$$U_\varepsilon \approx (\,U_e^{\,2} + U_m^{\,2}\,)^{\,½} \tag{1.3}$$

Quantification of the measurement (U_e) and model input (U_m) uncertainties is discussed in the chapters that follow.

The statistical normal significance test considers the difference of the mean values with known and unequal variances to be in agreement at a 95 % confidence level [Ref.10] if:

$$\left|\varepsilon\right| = \leq \left|U_\varepsilon\right| \tag{1.4}$$

where the distributions for U_e and U_m (about the mean values, ΔE and ΔM, respectively) are assumed to be Gaussian. The examination associated with Eq. 1.4 is analogous to asking if the expanded uncertainty bars in Figure 1.1 overlap. If Eq. 1.4 does not hold, then the difference between the model and measurement are not within the bounds of the combined expanded

uncertainty, U_ε. This may be due to a variety of reasons including issues not considered in the uncertainty analysis, such as measurement bias, uncharacterized experimental uncertainty, inappropriate application of a model, or intrinsic model uncertainty.

The hypothetical data shown in Fig. 1-1 and the data from all but one of the experimental series was time-averaged over a 10 s interval for use in this V&V study. The data in the NBS data set was acquired every 10 s with a 6 s time-average. A nearly-uniform value for the time-averaging interval establishes consistency among the various experimental data sets. The value of this interval is selected based on a desire to reduce the impact of experimental noise on the determination of ε (see Eq. 1.1), and the need to minimize data smoothing without loss of significant information. Appendix B provides example calculations regarding this issue.

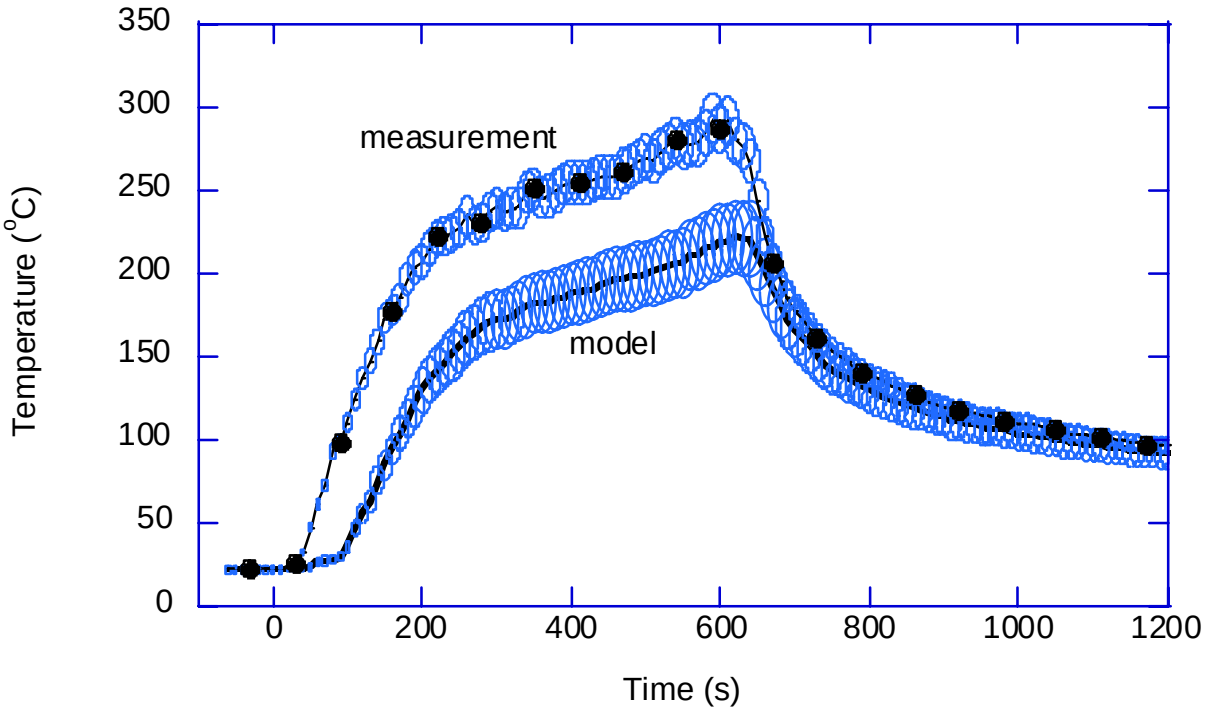

Figure 1-1: Comparison of hypothetical measured and simulated temperature profiles. Uncertainties associated with the measurements and model inputs are also shown.

1.5 Organization of this Volume

This volume is organized as follows:

- Chapter 2 defines the heat release rate and discusses uncertainty in its measurement, which is important the determination of the *model input uncertainty* (U_m, see Eq. 1.3), which is discussed in Chapter 5.
- Chapter 3 discusses each of the six experimental series considered in this report (see Table 1-1).

- Chapter 4 addresses the uncertainty in the experimental measurements, which is important in model evaluation and the determination of the *combined uncertainty* (U_e, see Eq. 1.3)
- Chapter 5 discusses the value of the model input uncertainty (U_m) for each of the measurements. For each parameter of interest, a simple analytic description of the sensitivity of that parameter to the fire heat release rate is given. The model input uncertainty (U_m) is estimated based on uncertainty in the experimental heat release rate, and a number of other parameters. The magnitude of this uncertainty plays an important role in the evaluation of model accuracy through consideration of Eq. 1.4 above.
- Chapter 6 summarizes the experimental (U_e) and model input (U_m) uncertainties taken from Chapters 4 and 5, respectively, and uses these values to calculate the combined uncertainty (see Eq. 1.3). The combined uncertainties are weighted and used to determine a representative uncertainty for comparison with ε, the relative difference between the measurements and the models.

Chapter 7 presents a list of references.

Appendix A provides documentation of personal communications cited in the text.

Appendix B presents a series of calculations addressing the interval used to time-average the data

2
MODEL INPUT AND ITS UNCERTAINTY

This chapter discusses model input and its uncertainty. Attention focuses primarily on the heat release rate (HRR), its measurement, and its uncertainty. The uncertainty in the HRR turns out to be the most significant *model input uncertainty.* The fire HRR is the single most important parameter in terms of characterizing a fire. The HRR controls the thermal impact of a fire on its environment. The current generation of fire models cannot accurately predict the transient HRR of a fire and for the fire model evaluations considered in this report, the HRR is prescribed. The sensitivity of model output to the HRR uncertainty is an important part of the model evaluation in this report series and is discussed in detail in Chapter 5.

The actual HRR of a fire ($\dot{Q}$) is a function of the mass loss rate of fuel ($\dot{m}$), the heat of combustion (H_c), and the combustion efficiency (χ_A):

$$\dot{Q} = \chi_A \ \dot{m} \ H_c \tag{2.1}$$

In some fire models, the radiative fraction of a fire is a model input. Since the radiative fraction was not reported in the documentation of the experiments considered in this report, this chapter suggests values for use in the model evaluation considered in this report series. The radiative fraction provides information on how the energy from a fire is distributed between the sensible enthalpy convected by the plume and the heat transferred to the surroundings by radiation. The radiative fraction, χ_{rad}, is based on the idealized HRR of a fire ($\dot{m} \ H_c$) and is defined as:

$$\dot{Q}_r = \chi_{rad} \ \dot{m} \ H_c \tag{2.2}$$

where $\dot{Q}_r$ is the radiative emission from a fire to its surroundings. As used in the fire literature (e.g., Ref. 11), the radiative fraction of a fire does not consider radiative exchange with walls or a hot upper layer.

2.1 Heat Release Rate Measurement Uncertainty

In the experiments considered in this report the heat release rate was determined by measuring the mass loss rate of fuel or by an oxygen consumption calorimetry measurement.

Calorimetric measurements typically involve dozens of independent measurements [Ref. 11], and a combined uncertainty analysis can be quite elaborate. Measurement uncertainty depends on the exact instrument types, details of the flow and sampling hardware, experimental procedures, and application details. Ref. [11] provides a survey of the few studies that address uncertainty of the HRR measurement by oxygen consumption calorimetry. These studies considered completely different situations including various types of instrumentation, different levels of the HRR, and detail of the analysis, including several versions of the HRR equation. Ref. [12] estimated the HRR measurement uncertainty for the measurement as conducted in the Single Burning Item Test and the Room Corner Test (ISO 9705). The relative expanded

uncertainty estimates ranged from 0.07 to 0.14, depending on the apparatus and the HRR. The uncertainty of the oxygen concentration measurement, followed by the heat of combustion factor and the mass flow rate measurement were identified as the major sources of uncertainty. Details on the uncertainty of the oxygen and the mass flow rate measurements were presented. The study notes that for larger oxygen deficits the combined uncertainty of the HRR measurement is less. Ref. [13] performed an analytical estimate of the HRR measurement uncertainty for the cone calorimeter. They estimated relative expanded uncertainty values from 0.10 to 0.12, depending on the HRR. The greatest sources of uncertainty were identified as the heat of combustion factor, the combustion expansion factor, and the oxygen measurement. Ref. [14] performed an uncertainty analysis for experiments conducted in a compartment with a controlled energy supply. The volume flow rate and oxygen measurement were identified as majors source of uncertainty, and a relative expanded uncertainty of 0.12 was reported under conditions when the exhaust volume flow rate was optimized for the fire size. The oxygen depletion measurement and the exhaust mass flow rate measurement have been consistently identified as major sources of uncertainty. Ref. [15] reviewed, however, the results of the HRR round-robin tests, and highlighted the uncertainty due to random effects, such as material and burning variability, environmental effects, operator error, and measurement bias between laboratories.

For some of the experiments considered here, the HRR was estimated through measurement of the fuel flow rate. In these cases, the HRR was calculated based on the heat of combustion and an assumed combustion efficiency (Eq. 2.1). While the mass flow rate measurements typically have low uncertainties, the uncertainty in the combustion efficiency is not necessarily small. Inside a compartment, even less is known about combustion efficiency as the fire plume is partially engulfed in a hot upper layer and the oxygen volume fraction in the lower layer is vitiated.

2.2 Radiative Fraction

The radiative fraction is typically determined through single or multiple location measurements of the radiative flux, $\dot{q}''$, at a significant distance from the fire in conjunction with a measurement of the mass burning rate, $\dot{m}$. Assuming symmetry, χ_{rad} can be determined either through single or multiple-location heat flux measurements at a suitable distance from the fire source. The radiative fraction of burning pools of hydrocarbons, such as those used in the experiments considered here, vary with fuel type [Ref. 16, 17] and scale of the fire [Ref. 18]. Measurement of the radiation from a fire should avoid reflection or re-radiation from nearby walls or partitions.

2.3 Summary of Results from the Experiments

The values of the HRR varied from experiment to experiment, depending on the nature of the experimental conditions. This information is available in the test reports [Refs. 2 through 6] and is summarized in Table 2-1. Table 2-1 also presents the values of the estimated uncertainty of the HRR for the six experiments, which varied from 15 % to 25 %. For two of the experiments considered here (BE #2 and BE #4), the HRR was estimated through the fuel flow rate measurement results. In these cases, the HRR was calculated based on Eq. 2.1 and data on the heat of combustion and the combustion efficiency. Whereas the mass flow rate measurement typically has low uncertainty, the uncertainty in the combustion efficiency is not necessarily

small. Inside a compartment, even less is known about combustion efficiency as the fire plume may be partially engulfed in a hot upper layer and the oxygen volume fraction in the lower layer may be vitiated. The table also lists values of the radiative fraction, and its uncertainty. Discussion of the table entries is given in detail in Chapter 3 for each of the six experimental test series.

Table 2-1: Summary of the Heat Release Rate and Radiative Fraction

Series	Test	Fire	Peak HRR (kW)	Radiative Fraction
FM/SNL Ref. [2]	Test 4	Propylene 0.9 m round sand burner	510 ± 20 %	0.35 ± 20 %
	Test 5		480 ± 20 %	
	Test 21		470 ± 20%	
NBS Ref.[3]	100A	natural gas	110 ± 15 %	0.20 ± 20 %
	100O	natural gas/acetylene gas burner	110 ± 20%	0.30 ± 30 %
	100Z		110 ± 20 %	0.30 ± 30 %
BE #2 Ref. [4]	Case 1	heptane on water round 1.17 m pan	Mass loss Uncertainty: ± 15%	0.35 ± 20 %
	Case 2	heptane on water round 1.60 m pan		
	Case 3			
BE #3 Ref. [5]	15 tests	heptane & toluene (1 test) spray round, 1 m ± 0.1 m diameter pool	400-2300; see Ref.[5] ± 17 % uncertainty	heptane: 0.44 ± 16 % toluene: 0.40 ± 23 %
BE #4 Ref. [6]	Test 1	jet fuel	Mass loss Uncertainty: ± 25%	0.35 ± 20 %
BE #5 Ref. [7]	Test 4	propane gas burner	see Fig. 3-9 Uncertainty: ± 15%	0.35 ± 20 %
		ethanol pan fire		0.20 ± 20 %

3
TEST SERIES

In this chapter, each of the six experimental series is described and certain measurements are discussed, most notably, the heat release rate (HRR) and the radiative fraction. The HRR and the radiative fraction varied from experiment to experiment, as did the uncertainty of these parameters. This information is summarized in Table 2-1 in Chapter 2.

Because measurement uncertainty was not documented for many of the experiments, engineering judgment is used, in this and the following chapter, to estimate its value. Measurements vary from experiment to experiment, and for each attribute being measured. The accurate determination of experimental uncertainty is challenging, and characterizing the uncertainty in experiments conducted by others is even more so. A good faith effort is made here to quantify measurement uncertainty, but the uncertainty determination provided in this document should be regarded as estimates and the uncertainty bounds presented here should be regarded as guidelines, to assist in the evaluation of the predictive capabilities of the models. Some factors that contribute to experimental uncertainty were not considered here, but may be important. For measurements, systematic error may have been present, but may have been unidentified. Human error is always present in the implementation of instrumentation and interpretation of measurement results. In this sense, it is recognized that the uncertainty values presented here are not necessarily all-inclusive or definitive. This highlights the importance of expert judgment in this study and in the interpretation of the agreement between measurements and models.

3.1 FM/SNL Test Series

The Factory Mutual and Sandia National Laboratories (FM/SNL) Test Series was a series of 25 fire tests conducted for the NRC by Factory Mutual Research Corporation (FMRC), under the direction of Sandia National Laboratories (SNL). The primary purpose of these tests was to provide data with which to validate computer models for various types of NPP compartments. The experiments were conducted in an enclosure measuring 60 ft long x 40 ft wide x 20 ft high (18 m x 12 m x 6 m), constructed at the FMRC fire test facility in Rhode Island. All of the tests involved forced ventilation to simulate typical NPP installation practices. The fires consisted of a simple gas burner, heptane or methanol liquid pools, or a polymethylmethacrylate (PMMA) solid fire. Four of the tests were conducted with a full-scale control room mockup in place. Parameters varied during the experiments included fire intensity, enclosure ventilation rate, and fire location. The FM/SNL test series is described in detail, including the types and locations of measurement devices, as well as some results in Refs. [2, 19, 20].

This V&V study used data from only three of the experiments (Tests 4, 5, and 21). In these tests, the fire source was a propylene gas-fired burner with a diameter of approximately 0.9 m (36 in), with its rim located approximately 0.1 m (4 in) above the floor. For Tests 4 and 5, a round 0.3 m (1 ft) diameter burner was centered along the longitudinal axis centerline, 6.1 m (20 ft) laterally from the nearest wall. For Test 21, the fire source was placed within a simulated benchboard electrical cabinet.

3.1.1 Heat Release Rate

The HRR was determined using oxygen consumption calorimetry in the exhaust stack with a correction applied for the CO_2 in the upper layer of the compartment. The uncertainty of the fuel mass flow was not documented. All three tests selected for this study had the same target peak heat release rate (HRR) of 516 kW following a 4 min "t-squared" growth profile. The test report contains time histories of the measured HRR, for which the average sustained HRR following the ramp up for Tests 4, 5, and 21 have been estimated as 510 kW, 480 kW, and 470 kW, respectively. Once reached, the peak HRR was maintained essentially constant for another 6 min (Tests 4 and 5) and 16 min (Test 21). Figure 3-1 shows the prescribed and measured HRR as a function of time during Test 21 of the FM/SNL test series. Even though time-dependent curves are reported in Ref. [20], it was decided to use averaged values during the steady phase, because it is assumed that the fuel flow would have been held steady during this period, and that fluctuations in HRR are expected from calorimetry measurements. It was noted in the test report that during Tests 4, 5, and 21 there was a downward bias in the measured HRR due to "significant" loss of effluent from the exhaust hood. This bias was treated as an additional uncertainty, and the relative combined expanded uncertainty was assumed to equal ±20 %, which is somewhat larger than typical calorimetric measurement uncertainty.

3.1.2 Radiative Fraction

The radiative fraction (see definition in Chapter 2) was not measured for propylene, but it is assumed to equal 0.35 which is typical for smoky hydrocarbons [Ref. 17]. The expanded uncertainty in this value was taken as ± 20 %, a value typical of reported uncertainty [21, 22]. It was further assumed that the radiative fraction was about the same in Test 21 as the other tests, as fuel burning must have occurred outside of the electrical cabinet in which the burner was placed.

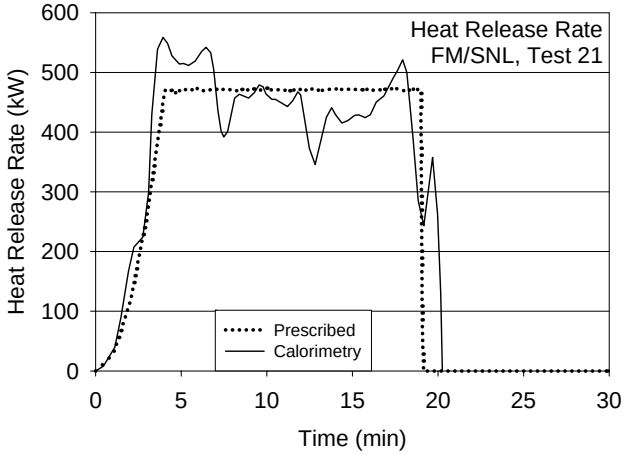

Figure 3-1: Prescribed and measured heat release rate as a function of time during Test 21 of the FM/SNL test series

3.1.3 Other Measurements

As seen in Table 1-2, four types of measurements were conducted during the FM/SNL test series and used in the evaluation conducted here, including the HGL temperature and depth, and the temperatures of the ceiling jet and the plume. Aspirated thermocouples were used to make all of these measurements. The aspirated thermocouple (TC) measurements presented in this study are preferable to bare-bead TC measurements, as radiative exchange measurement errors are reduced. For the relatively low temperatures observed (~100 ^{o}C), however, the differences are expected to be small.

Aspirated Thermocouples: Aspirated thermocouple measurements for the range of temperatures measured are typically accurate to about 10 °C (13 °F); see the discussion of thermocouple uncertainty in Chapter 4. The temperatures were measured using the aspirated thermocouples in Sectors 1, 2 and 3, plus the near-ceiling TCs directly above the burner in Test 4 and 5.

HGL Depth and Temperature: Data from all of the vertical thermocouple trees were used when reducing the HGL height and temperature. For the FM/SNL Tests 4 and 5, Sectors 1, 2 and 3 were used, all weighted evenly. For Test 21, Sectors 1 and 3 were used, evenly weighted. Sector 2 was partially within the plume in Test 21.

3.2 NBS Multi-Compartment Test Series

The National Bureau of Standards (NBS, which is now the National Institute of Standards and Technology, NIST) Multi-Compartment Test Series consists of 45 fire tests representing 9 different sets of conditions, with multiple replicates of each set, which were conducted in a three-room suite described in detail in Ref. [3]. The suite consisted of two relatively small rooms, connected via a relatively long corridor. The fire source, a gas burner, was located against the rear wall of one of the small compartments. Fire tests of 100 kW, 300 kW and 500 kW were conducted. For the current V&V study, only three 100 kW fire experiments have been used, including Test 100A from Set 1, Test 100O from Set 2, and Test 100Z from Set 4. The selected data are also available in Ref. [23].

For the NBS Multi-room series, Tests 100A, 100O and 100Z were used because they were constructively used in a previous EPRI study [Ref. 23]. The data in the NBS data set was acquired every 10 s with a 6 s time-average. This time-averaging interval was somewhat smaller than all of the other experimental series, which were time-averaged over a 10 s interval.

3.2.1 Heat Release Rate

Figures 3-2 and 3-3 show the experimentally measured HRR as a function of time during Tests 100A and 100 Z, respectively, of the NBS multi-room test series. In these two tests, for which the door was open, the measured HRR via oxygen consumption calorimetry was taken to be 110 kW ±17 kW (±15 %). The combined relative expanded (2σ) uncertainty in the calorimetric HRR is assigned a value of ±15 %, consistent with the replicate measurements made during the experimental series and the uncertainty typical of oxygen consumption calorimetry. This value is also consistent with the measurement variation seen in the figures. It was assumed that the closed door test (Test 100O) had the same HRR as the open door tests.

The prescribed HRR is also shown in the figures. The prescribed HRR is nominally the value of the HRR in the compartment (unless the fire is underventilated, which was not the case in these experiments). The prescribed HRR differs from the measured value in the exhaust hood due to mixing in the upper layer of the compartment, which effectively adds a time-response function to the measurement. The prescribed HRR has been inferred from the calorimetric measurement made in the exhaust hood. As expected, the measured HRR increased slowly with time, and then approached the prescribed value, which was intended to be steady

The mass flow of the fuel (natural gas in Test 100 A, or natural gas mixed with acetylene in Tests 100O and 100Z) was not metered; rather, the effluent was captured in a hood mounted above the open door in the corridor and the HRR was measured using oxygen consumption calorimetry. The manner by which the fuel flow was controlled is not documented. In Test 100, candles were used to increase smoke in the upper layer to allow visualization. Tests 100 O and 100Z used acetylene (about 20 % by volume) to produce smoke. In those tests, the flow of natural gas and acetylene were adjusted to obtain approximately the same HRR as in Test 100A.

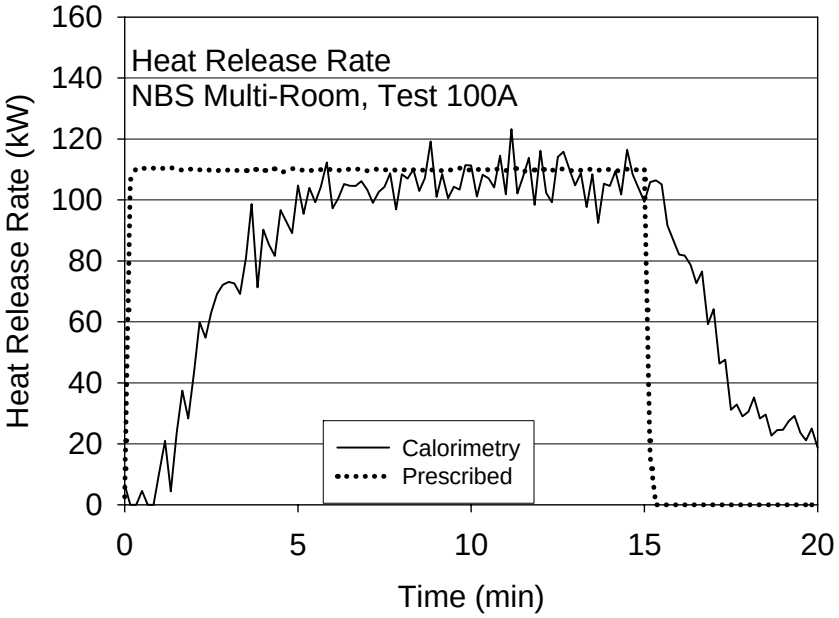

Figure 3-2: Prescribed and measured heat release rate as a function of time during Test 100A of the NBS multi-room test series.

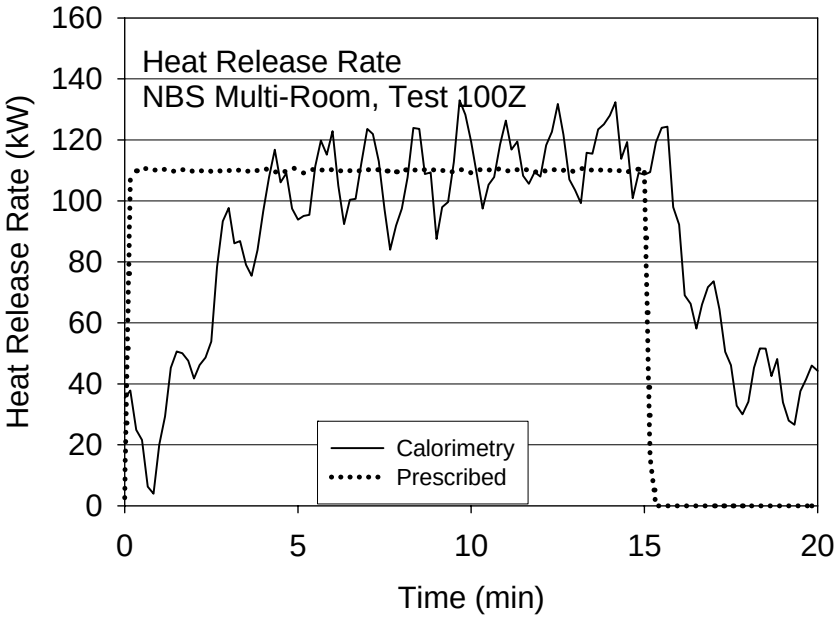

Figure 3-3: Prescribed and measured heat release rate as a function of time during Test 100Z of the NBS multi-room test series.

The addition of acetylene increased the radiative fraction of the fire, which is discussed in the next section.

3.2.2 Radiative Fraction

For many reasons, natural gas supplied by large utility companies is often used in fire experiments. While its composition may vary from day to day, there is little change expected in the value of the radiative fraction. As mentioned above, natural gas was used as the fuel in Test 100A. In Tests 100O and 100Z, acetylene was added to the natural gas to increase the smoke yield, and as a consequence, the radiative fraction increased. The radiative fraction of natural gas has been studied previously, whereas the radiative fraction of the acetylene/natural gas mixture has not been studied. The radiative fraction for the natural gas fire was assigned a value of 0.20, whereas a value of 0.30 was assigned for the natural gas/acetylene fires [Ref. 11].

The relative combined expanded (2σ) uncertainty in this parameter was assigned a value of ±20 % in Test 100A and ±30 % in 100O and 100Z. The 20 % expanded deviation value is consistent with typical values of the deviation reported in the literature for the measured radiative fraction. The 100O and 100Z tests had a 50 % larger value assigned, because the effect on the radiative fraction of adding acetylene to the natural gas was not measured.

3.2.3 Other Measurements

Measurements made during the NBS test series included gas and surface temperature, pressure, smoke and major gas species concentration, and doorway gas velocity. As seen in Table 1-2, only two types of measurements conducted during the NBS test series were used in the evaluation considered here. These were the HGL temperature and depth, in which bare bead thermocouples were used to make these measurements. Single point measurements of temperature within the burn room were not used in the evaluation of plume or ceiling jet algorithms. This is because, in neither instance, was the geometry consistent with the assumptions used in the algorithms. Specifically, the burner was mounted against a wall, and the room width to height ratio was less than that assumed by the various ceiling jet correlations.

3.3 ICFMP Benchmark exercise #2

The experiments are described in Ref. [4]. Benchmark Exercise #2 (BE #2) consisted of 8 experiments, representing 3 sets of conditions, to study the movement of smoke in a large hall with a sloped ceiling. The results of the experiments were contributed to the International Collaborative Fire Model Project (ICFMP) for use in evaluating model predictions of fires in larger volumes representative of turbine halls in NPPs. The tests were conducted inside the VTT Fire Test Hall, which has dimensions of 19 m (62 ft) high by 27 m (89 ft) long by 14 m (46 ft) wide. Each case involved a single heptane pool fire, ranging from 2 MW to 4 MW.

As seen in Table 1-2, four types of measurements conducted during the VTT test series (BE #2) were used in the evaluation considered here, including the HGL temperature and depth, average flame height and the plume temperature. Three vertical arrays of thermocouples, plus two plume thermocouples, were used. The HGL temperature and height were reduced from an average of the three TC trees using the standard algorithm. No ceiling jet evaluation was done because the ceiling in the test hall is not flat.

3.3.1 Supplementary Information

The VTT test report lacks some information that is needed to model the experiments, so some information was based on private communications with the principal investigator [Ref. 24].

Surface Materials: The walls and ceiling of the test hall consist of a 1 mm (0.039 in) thick layer of sheet metal on top of a 5 cm (2 in) layer of mineral wool. The floor was constructed of concrete. The report does not provide thermal properties of these materials.

Natural Ventilation: In Cases 1 and 2, all doors were closed, and ventilation was restricted to infiltration through the building envelope. Precise information on air infiltration during these tests is not available. The scientists who conducted the experiments recommend a leakage area of about 2 m^2 (20 ft^2), distributed uniformly throughout the enclosure. By contrast, in Case 3, the doors located in each end wall (Doors 1 and 2, respectively) were open to the external ambient environment. These doors are each 0.8 m (2.6 ft) wide by 4 m (5 ft) high, and are located such that their centers are 9.3 m (30.5 ft) from the south wall.

Mechanical Ventilation: The test hall has a single mechanical exhaust duct, located in the roof space, running along the center of the building. This duct has a circular section with a diameter of 1 m (40 in), and opens horizontally to the hall at a distance of 12 m (39 ft) from the floor and 10.5 m (34.4 ft) from the west wall. Mechanical exhaust ventilation was operational for Case 3, with a constant volume flow rate of 11 m^3/s drawn through the 1 m (40 in) diameter exhaust duct.

HGL height and Temperature: All of the vertical thermocouple trees were used to compute the HGL depth and temperature, with all of the trees evenly weighted.

3.3.2 Heat Release Rate

Each test used a single fire source with its center located 16 m (52 ft) from the west wall and 7.4 m (24.3 ft) from the south wall. For all tests, the fuel was heptane in a circular steel pan that was partially filled with water. The pan had a diameter of 1.17 m (46.0 in) for Case 1 and 1.6 m (63 in) for Cases 2 and 3. In each case, the fuel surface was 1 m (40 in) above the floor. The trays were placed on load cells, and the HRR was calculated from the mass loss rate (see

definition in Chapter 3). For the three cases, the fuel mass loss rate was averaged from individual replicate tests. However, the HRR was not measured, and must be inferred from the mass loss data. Thus, the HRR in BE #2 was based on the mass burning rate measurement (see Chapter 2).

In the HRR calculation, the heat of combustion for n-heptane was used (44.6 kJ/g). Hostikka [Ref. 4] suggests a value of 0.8 for the combustion efficiency, which is a compromise between 0.7 [Ref.17] and various other estimates around 0.9. Bundy [Ref. 25] put the efficiency of a 500 kW heptane fire as high as 0.97. The magnitude of the combustion efficiency is a complicated function of fire size and other effects. The combustion efficiency tends to decrease as the fire gets larger, and compartment effects are not well understood. In this report, a combustion efficiency of 0.85 ± 0.12 (or ± 14 %) is recommended, based on engineering judgment. Given the range of values associated with the value of χa, the uncertainty in the HRR is dominated by uncertainty in the combustion efficiency. Uncertainty in the mass loss rate measurement also contributes, so the uncertainty in the HRR was estimated as 15 %. Figures 3-4 to 3-6 show the prescribed HRR as a function of time during Cases 1 to 3, respectively, during the ICFMP BE #2 test series. Tables 3-1 to 3-3 represent the mass loss and estimated HRR associated with Figures 3-4 to 3-6, respectively.

3.3.2 Radiative Fraction

The radiative fraction was assigned a value of 0.30, similar to many smoky hydrocarbons [Ref. 17]. The relative combined expanded (2σ) uncertainty in this parameter was assigned a value of ±20 %, typical of uncertainty reported in the literature for this parameter.

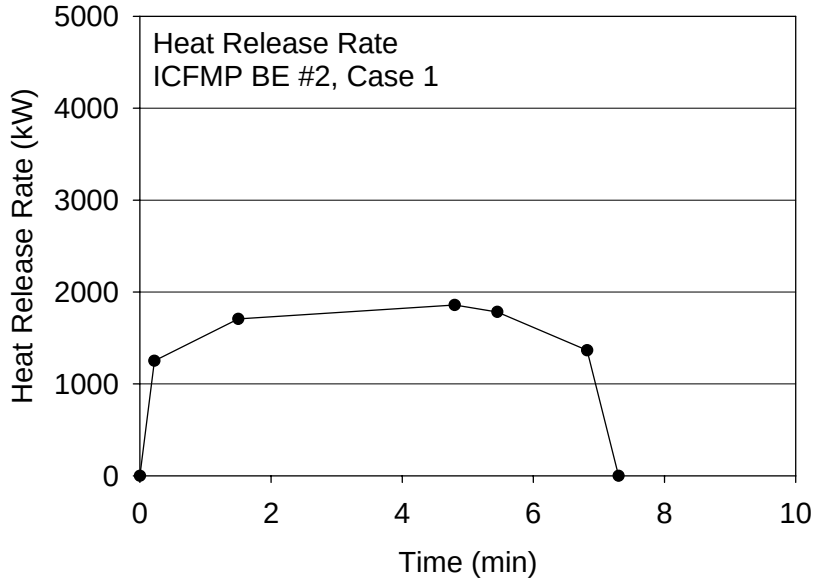

Figure 3-4: Prescribed heat release rate as a function of time during Case 1 of the BE #2 test series.

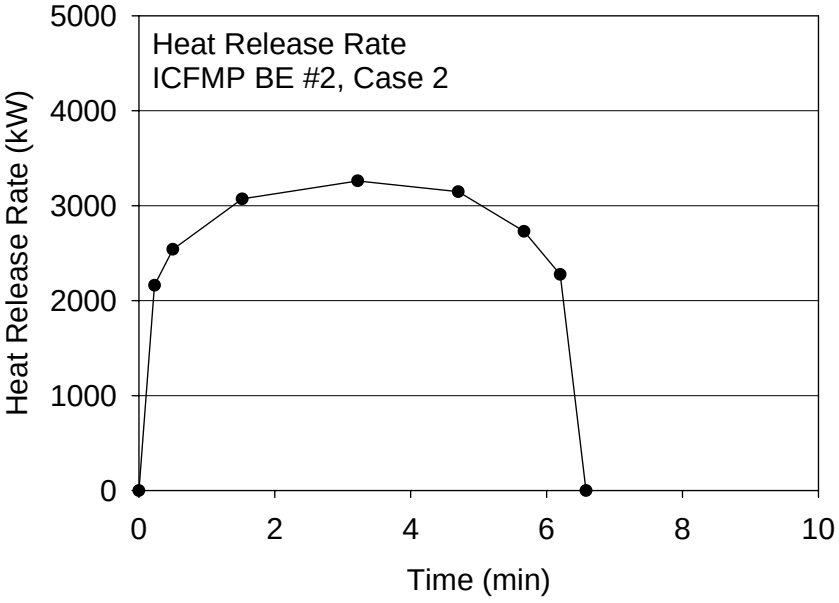

Figure 3-5: Prescribed heat release rate as a function of time during Case 2 of the BE #2 test series.

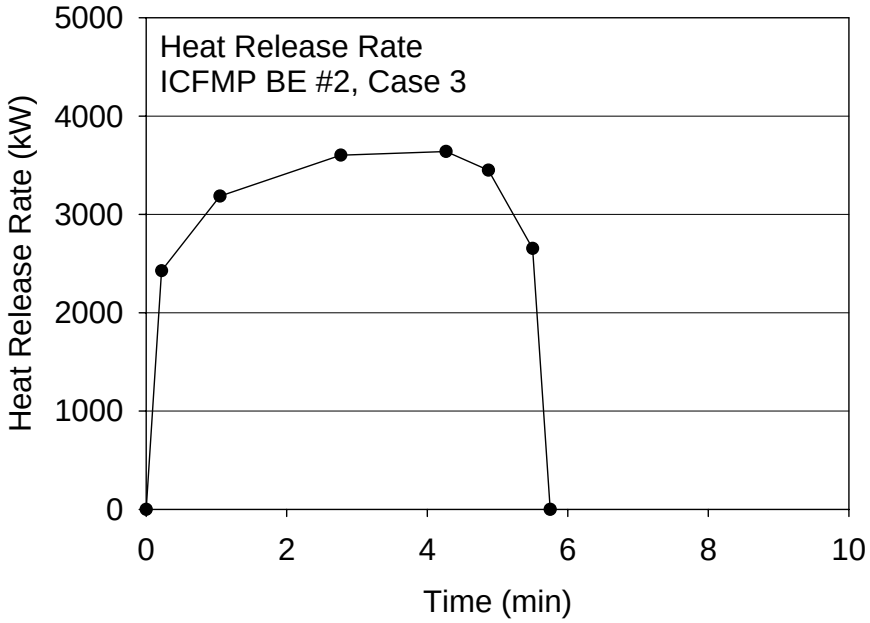

Figure 3-6: Prescribed heat release rate as a function of time during Case 3 of the BE #2 test series.

Table 3-1: Mass Loss and Heat Release Rates for Case 1 of the BE #2 test series

Time (s)	MLR (kg/s)	HRR (kW)
0	0	0
13	0.033	1250
90	0.045	1706
288	0.049	1857
327	0.047	1782
409	0.036	1364
438	0	0

Table 3-2: Mass Loss and Heat Release Rates for Case 2 of the BE #2 test series

Time (s)	MLR (kg/s)	HRR (kW)
0	0	0
14	0.057	2161
30	0.067	2540
91	0.081	3071
193	0.086	3261
282	0.083	3147
340	0.072	2729
372	0.060	2275
395	0	0

Table 3-3: Mass Loss and Heat Release Rates for Case 3 of the BE #2 test series

Time (s)	MLR (kg/s)	HRR (kW)
0	0	0
13	0.064	2426
63	0.084	3184
166	0.095	3601
256	0.096	3639
292	0.091	3449
330	0.070	2654
345	0	0

3.4 ICFMP Benchmark Exercise #3

Benchmark Exercise #3, conducted as part of the International Collaborative Fire Model Project (ICFMP) and sponsored by the NRC, consisted of 15 large-scale experiments performed at NIST in June 2003. The experiments are documented in Ref. [5]. The fire sizes ranged from 350 kW to 2.2 MW in a compartment with dimensions 21.7 m x 7.1 m x 3.8 m high, designed to represent a compartment in a NPP containing power and control cables. Walls and ceiling were covered with two layers of marinate boards, each layer 0.0125 m (½ in) thick. Thermophysical properties of the marinate and other materials are given in Ref. [5]. The floor was covered with one layer of 0.0125 m (½ in) thick gypsum board on top of a 0.0183 m (23/32 in) layer of plywood. The room had one door and a mechanical air injection and extraction system. Ventilation conditions, the fire size, and fire location were varied, and the numerous experimental measurements included gas and surface temperatures, heat fluxes, and gas velocities.

3.4.1 Supplementary Information

Natural Ventilation: The compartment had a 2 m x 2 m door in the middle of the west wall. Some of the tests had a closed door (Tests 4, 10, 16, and 17), and in those tests compartment leakage was a very important parameter. Ref. [5] reports leakage area based on measurements performed prior to Tests 1, 2, 7, 8, and 13. For the closed door tests (Tests 4, 10, 16, and 17), the leakage areas ought to be based on the last available measurement. It should be noted that the chronological order of the tests differed from numerical order [Ref. 5]. For Test 4, it is recommended that the leakage area measured before Test 2 be used. For Tests 10 and 16, it is recommended that the leakage area measured before Test 7 be used.

Mechanical Ventilation: Mechanical ventilation and exhaust was used during Tests 4, 5, 10, and 16, providing about 5 air changes per hour. The supply duct was positioned on the south wall, about 2 m off the floor. An exhaust duct of equal area to the supply duct was positioned on the opposite wall at a comparable location. The flow rates through the supply and exhaust ducts were measured in detail during breaks in the testing, in the absence of a fire.

During the tests, the flows were monitored with single bi-directional probes during the tests themselves. A bi-directional probe was positioned in the center of the exhaust duct, and its velocity was recorded under the column header “BP Exhaust Vent” in the BE #3 experimental data sets. Its value varied between 3 m/s (10 ft/s) and 4 m/s (13 ft/s) for the four ventilated tests. The supply and exhaust volume flow rates and other pertinent information can be found in Ref. [5]. Usually this is expressed as the vent area times an average velocity. Another bi-directional probe was positioned in the supply duct, 30 cm (1 ft) from the bottom of the duct during Tests 4 and 5, and 15 cm from the bottom of the duct for Tests 10 and 16. In the data sets, this measurement is listed under the column header “BP Supply Vent-16”. Its value was between 3 m/s (10 ft/s) and 4 m/s (13 ft/s) for Tests 4 and 5, and was as high as 10 m/s (33 ft/s) during Tests 10 and 16.

The exhaust duct profile was relatively uniform, whereas the supply was not. Most of the air was blown out of the bottom third of the supply duct. The single point measurements during the fire tests indicated that the flow field changed from its ambient values. The measured supply volume flow rate of 1.06 m^3/s (37.4 ft^3/s) pre-test decreased to 0.9 m^3/s (31 ft^3/s) during testing. For the exhaust, the measured volume flow rate of 1.03 m^3/s (36.4 ft^3/s) pretest increased to

about 1.7 m^3/s (60 ft^3/s) during testing. The uncertainties during the fires are substantially higher than the uncertainties in the ambient measurements (±0.2 m^3/s or 7 ft^3/s). Doubling this value is appropriate.

The ventilation system affected the compartment pressure, HGL temperature, and the surface temperature of various cable targets. The cable surface TCs were just outside of the direct path of the supply fan. In the absence of a fire, blowing was observed to flow upwards at about a 35° angle.

Fuel Delivery: The fire was located at floor level in the center of the compartment for most of the tests (Tests 1 - 13, 16, and 17). In Test 14, the fire was centered 1.8 m (72 in) from the North wall. In Test 15, the fire was centered 1.25 m (50 in) from the South wall. In Test 18, the fire was centered 1.55 m (62 in) from the South wall. Physically, the fuel pan was 2 m (80 in) long x 1 m (40 in) wide and 0.1 m (4 in) deep. A single nozzle was used to spray liquid hydrocarbon fuels onto a 1 m (40 in) by 2 m (80 in) fire pan that was about 0.02 m deep (1 in). The test plan originally called for the use of two nozzles to provide the fuel spray. Experimental observation suggested that the fire was less unsteady with the use of a single nozzle. In addition, it was observed that the actual extent of the liquid pool was well-approximated by a 1 m (40 in) circle in the center of the pan. The uncertainty in the location of the liquid fuel was about ±0.1 m (± 4 in). For safety reasons, the fuel flow was terminated when the lower-layer oxygen concentration dropped to approximately 15% by volume.

3.4.2 Heat Release Rate

The fuel used in 14 of the tests was heptane, while toluene was used for one test (Test 17). The HRR was determined using oxygen consumption calorimetry. The uncertainty in the HRR measurement was documented in Ref. [5]. The recommended uncertainty values were 17 % for all of the tests. Figure 3-7 shows the measured and prescribed HRR as a function of time during Test 3. Ref. [5] discusses the shape of the prescribed HRR curve in detail.

3.4.3 Radiative Fraction

The radiative fraction was measured in an independent study for the same fuels using the same spray burner as used in the BE #3 test series [Ref. 21]. The value of the radiative fraction and its uncertainty were reported as 0.44 ± 16 % and 0.40 ± 23 % for heptane and toluene, respectively (also see Table 2-1.).

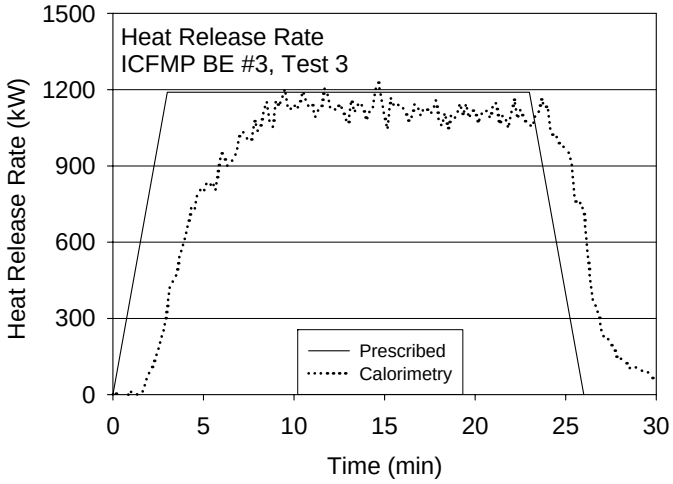

Figure 3-7: Measured and prescribed heat release rate as a function of time during Test 3 of the ICFMP #3 test series.

3.4.4 Other Measurements

As seen in Table 1-2, measurements made during the NIST test series (BE #3) included all 13 parameters considered in this study, except the plume temperature.

The vertical thermocouple trees were used to determine the HGL depth and temperature, except Tree 4, which had a faulty TC. The thermocouple data was weighted based on the location of the thermocouple tree in the compartment, and the portion of the area that was represented by the data from each tree. Table 3-4 shows the relative weightings. Trees 1 and 7 were weighted 0.3 each, Tree 2 was weighted 0.2, Tree 3 was weighted 0.1, and the others were weighted 0.05.

Table 3-4: Relative Weighting of the Calculation of HGL

Thermocouple Tree	Relative Weight
1	0.3
2	0.2
3	0.1
4	0
5	0.05
6	0.05
7	0.3

3.5 ICFMP Benchmark Exercise #4

Benchmark Exercise (BE) #4 consisted of kerosene pool fire experiments conducted at the Institut für Baustoffe, Massivbau und Brandschutz (iBMB) of the Braunschweig University of

Technology in Germany. The results of two experiments were contributed to the International Collaborative Fire Model Project (ICFMP) and documented in the report, *Evaluation of Fire Models for Nuclear Power Plant Applications: Fuel Pool Fire inside a Compartment* [Ref. 6]. These experiments involved relatively large fires in a relatively small (3.6 m x 3.6 m x 5.7 m high or 12 ft x 12 ft x 19 ft) concrete enclosure. Only Test 1 was selected for consideration in the present V&V study, because a significant amount of data was lost in Test 1, and the measured HRR during Test 3 exhibited significant amounts of fluctuation. As seen in Table 1-2, five types of measurements conducted during the BE #4 test series were used in the evaluation conducted here, including the HGL temperature and depth, temperature of targets and compartment surfaces, and heat flux.

3.5.1 Heat Release Rate

The fire in Test 1 was a 1 m x 1 m (40 in x 40 in) square pan of jet fuel, type A-1. Ref. [6] reports that the fuel is a mixture of hydrocarbons with a summary formula as $C_{11.64}H_{25.29}$, and that the thermophysical properties of the jet fuel were similar to dodecane [Ref. 6].

Figure 3-8 shows the heat release rate, which was estimated from the mass loss rate measurement. Table 3-5 lists the measured mass loss rate, as well as the calculated HRR, in which the heat of combustion and the combustion efficiency were taken as 42.8 MJ/kg and 1, respectively, as suggested by Ref. [6]. There were several reported difficulties in measuring the mass loss rate, including data loss due to an instrument malfunction and significant fluctuations in the measured mass loss rate. Due to the measurement issues and because the combustion efficiency was not well-characterized, the HRR uncertainty was assigned a relatively large expanded uncertainty of ±25 %.

Table 3-5: Measured Mass Loss Rate and Calculated

Time (s)	Mass Loss Rate (kg/s)	HRR (kW)
0	0	0
92	0.0028	119
180	0.037	1583
260	0.0613	2623
600	0.0747	3197
822	0.0783	3351
870	0.079	3381
1368	0.0822	3518

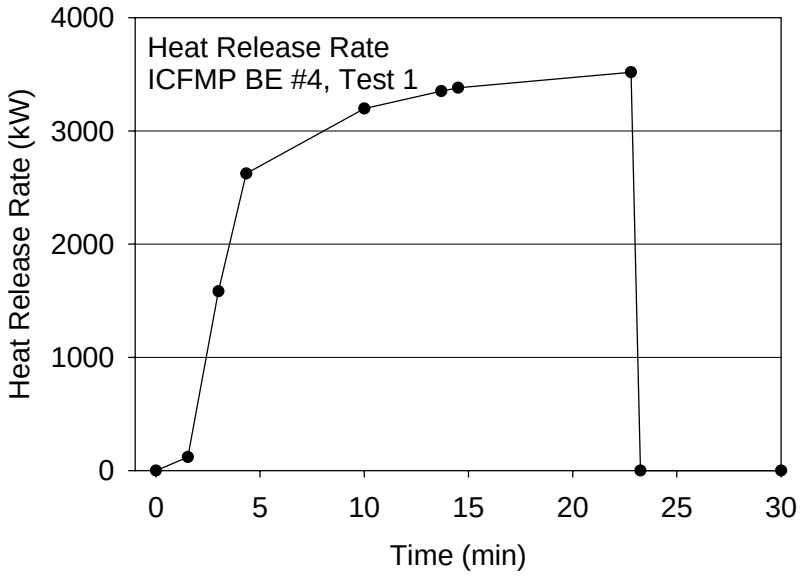

Figure 3-8: The estimated HRR based on the mass loss rate as a function of time during Test 1 of the BE #4 test series.

3.5.2 Radiative Fraction

The radiative fraction of the jet fuel was taken as 0.35, similar to other smoky hydrocarbons [Ref. 17]. The relative combined expanded uncertainty in this parameter was assigned a value of ±20 %, consistent with typical values reported in the literature for the measured radiative fraction [Refs. 19, 20].

3.6 ICFMP Benchmark Exercise #5

Benchmark Exercise (BE) #5, conducted under the International Collaborative Fire Model Project (ICFMP), comprised a series of four large-scale tests inside a concrete enclosure with realistically routed cable trays [Ref.7]. This test series was conducted at the Institut für Baustoffe, Massivbau und Brandschutz (iBMB) of the Braunschweig University of Technology in Germany. Test 4 of this test series was selected for the quantitative V&V study documented in this report.

As seen in Table 1-2, six types of measurements conducted during the BE #5 test series were used in the evaluation conducted as part of this report series, including the HGL temperature and depth, oxygen gas concentration, the temperature of targets and compartment surfaces, and heat flux.

3.6.1 Heat Release Rate

The fire involved a large fire in a relatively small enclosure. The first part of the selected test consisted of preheating the cable trays in the room. A 1 m^2 (11 ft^2) round pan on the floor filled with ethanol (ethyl alcohol) was used as the pre-heating source, and a propane gas burner was used as the fire source after pre-heating.

Exhaust products were collected in an exhaust duct and the HRR was measured using the oxygen calorimetry. For the purpose of this V&V study, the measured HRR was used as direct input to the various fire models. The first 20 min of data were used for the model evaluation. After 20 min, the HRR became relatively noisy. At 33 min, thermoplastic cables located in the compartment began to burn and contribute to the HRR. Figure 3-9 depicts the measured HRR profile. The relative combined expanded uncertainty in this parameter was assigned a value of ±15 %, consistent with typical values of this parameter [Ref. 11].

3.6.2 Radiative Fraction

The radiative fractions for the ethanol pool fire and the propane fire were taken as 0.20 and 0.35, respectively. The relative combined expanded uncertainty in this parameter was assigned a value of ±20 %, which is consistent with typical values reported for this parameter [Ref. 21, 22].

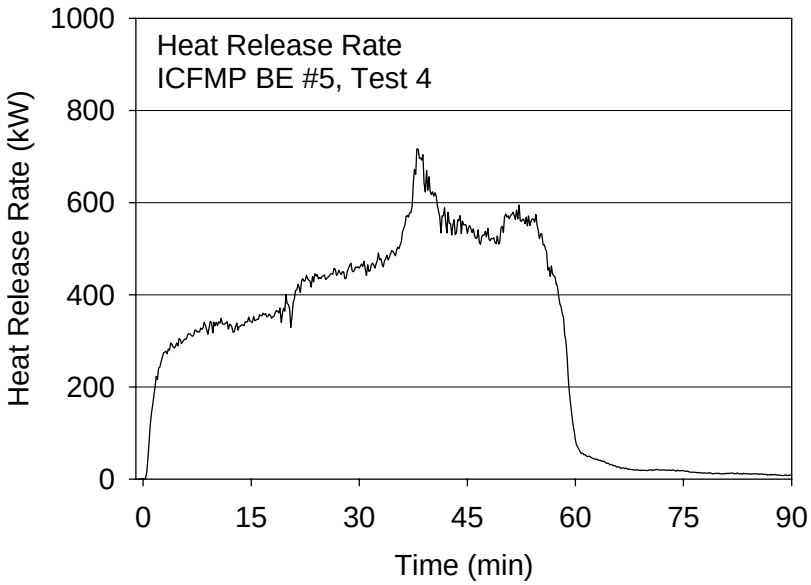

Figure 3-9: The heat release rate as a function of time during Test 4 of the BE #5 test series. Only the first 20 min of the test were used for model evaluation.

4
MEASUREMENT UNCERTAINTY

For many of the experiments and most of the measurements considered in this report, the experimental uncertainty was not documented. In this chapter, estimates of measurement uncertainty based on engineering judgment are provided. Quantifying uncertainty in measured quantities provides a basis for evaluation of model results through consideration of Eqs. 1.1 to 1.4. Documentation of the measurement uncertainty produces a consistent set of data for use in the evaluation of the models considered in this report. The uncertainty (U_e) of each of the 13 measurements considered in the model evaluation is provided (see Section 1.2 for a list of parameters, which included the hot gas layer temperature and depth, the ceiling jet and plume temperature, etc.).

The uncertainty estimates provided here are limited by knowledge of the details associated with each of the experiments. For this reason, the uncertainty values provided here should be thought of as rough estimates, rather than precise determinations of measurement uncertainty. Even for the experimentalists themselves, the accuracy of an uncertainty analysis is often limited by incomplete understanding. For example, in heat flux gauges, the uncertainty due to soot deposition on the face of the gauge is difficult to quantify. The amount of soot deposition depends on many parameters, such as the location of the gauge, the flow field and the temperature field near the gauge, the duration of the test, and the local soot volume fraction. Unexpected events or poor understanding limits the accuracy of an uncertainty analysis.

In general, measurement uncertainty depends on many issues, including the exact type of instrumentation, the experimental procedure, and the details of the measurement scenario. The uncertainty in many of the experimental measurements is difficult to accurately estimate, because most of the test reports do not provide uncertainties for the individual measurements. For this reason, the values are inferred based upon engineering judgment and experience with similar instrumentation.

4.1 Temperature and Hot Gas Layer Depth

The gas phase temperature was measured in all six of the experiments considered in this report. Thermocouples were used to characterize the depth of the hot gas layer (HGL) and the local temperature. Measurements were typically made at several vertical locations at one or more horizontal locations. Bare bead thermocouples were used in all of the experiments considered in this report except the BE #3 and FM/SNL tests in which bare and aspirated thermocouples were used. The HGL temperatures and depths were determined using the reduction method described by Peacock and Babrauskas [Ref. 26].

The interpretation of a bare bead thermocouple signal must consider several possible sources of error. Thermocouple (TC) measurement error can occur due to breakdown of the TC insulation at high temperatures, corrosion from acid combustion byproducts, decalibration at high temperatures, inherent measurement accuracy limited by materials effects, and measurement

error due to radiative exchange effects. The latter requires attention for the experiments considered in this report.

Blevins [Ref. 27] reported on the development of a model to compute TC error due to radiative exchange effects. Radiative exchange between the thermocouple and walls, flame gases, soot, and the ambient environment were considered. In the same document, report of soot accumulation on the TC bead or sensing junction and changing of its thermophysical properties may also contributing to error. Variability in the convective heat transfer between the sample gas and the TC junction is also cited as a source of error.

There are several ways to handle radiative exchange effects on TC measurements. A correction may be applied to the signal to improve measurement accuracy. This is burdensome, because the radiative exchange correction may depend on the character of the thermocouple, such as its diameter, its material composition, its surface emissivity, as well as the details of its application, involving the local temperature, radiation, and flow fields. So, the correction depends on local conditions, and each TC should be independently analyzed. Typically, not enough experimental information is available to perform an accurate radiation correction. In such a case, it may be more practical to expand the uncertainty bounds for the measurement to encompass radiative exchange effects that are estimated based on simplified assumptions. This approach is used here and described below.

A completely different measurement approach involves the use of an aspirated TC as the measurement device, in which radiative exchange effects are minimized. Aspirated TCs are constructed, such that the TC junction is within two concentric steel tubes. A mechanical pump draws gas extracted from the sampling location through a tube, engulfing the TC sensing junction with the sample gas, while the tubes protect the TC sensing junction from impinging thermal radiation. The error associated with the aspirated probe measurement itself depends on the application conditions and the results are a strong function of the aspiration velocity as well as a number of other parameters [Ref. 27, 28]. Aspirated thermocouples provide accurate temperature information, but typically are used sparingly, due to their relatively high cost compared to bare bead thermocouples. FM/SNL used aspirated TCs in the experiments considered in this report and BE #3 used aspirated TCs to assess the accuracy of the bare bead TC results.

In a hot upper layer of a compartment with lots of soot, a TC reading may be fairly accurate and not need to be corrected for radiative exchange effects. This is because the environment in such a scenario is nearly optically thick, for which radiative exchange effects are minimized. Many reports, including Refs.[2, 29, 30], have examined the magnitude of the TC measurement error due to radiative exchange by comparing bare bead TC measurements to measurements by nearby aspirated thermocouples in well-developed hot (60 ^{o}C to 800 ^{o}C; or 140 ^{o}F to 1500 ^{o}F) smoky upper layers of compartment fires. For the fires considered in this report, it is assumed that the upper layer in all of the tests had a high opacity at the time of the peak temperature readings. This is a reasonable assumption for the types of fuels being used in the experiments considered here with the exception of NBS Test 100A in which natural gas was used as a fuel. For the other tests, Table 2-1 shows that the fuels included smoky fuels such as toluene, heptane, propylene, jet fuel, and propane. Estimation of the uncertainty in the bare bead TC measurements involves determination of the uncertainty of the various components of the measurement and the effect that each component has on the overall uncertainty. Computation of the overall uncertainty

considers the measurement error due to radiative exchange, the inherent uncertainty associated with a bare-bead thermocouple, and the error associated with use of an aspirated thermocouple. The manufacturer reported accuracy for Type K TCs is 1.1 °C (2.0 °F) for temperatures between 0 °C (32 °F) and 293 °C (560 °F), and 0.4 % between 293 °C (560 °F) and 1250 °C (2280 °F), interpreted here as the expanded uncertainty [Ref. 31]. These values are listed in Table 4-1 as U_w for a number of temperatures. The expanded uncertainty associated with the aspirated probe measurement (U_a) is taken as approximately 4 % for an aspiration velocity of 15 m/s to 20 m/s as used in BE #3 [Ref. 27]. The value of U_a, listed in Table 4-1, also includes the inherent thermocouple uncertainty. The contribution of the uncertainty due to radiative exchange on a bare bead TC is estimated from the results of Refs. [2, 29, 30]. In those experiments, the measurement results of bare bead TCs were within 3 °C (5 °F) to 15 °C (27 °F) of nearby aspirated thermocouples. In the three FM/SNL tests [Ref. 2], for example, a bare bead thermocouple in the upper layer was within 5 °C (9 °F) to 6 °C (11 °F) of a nearby aspirated thermocouple, for upper layer temperatures of about 60 °C (140 °F). In a hot upper layer of a heptane fire [Ref. 29], bare bead thermocouples in the HGL were within 12 °C (22 °F) of nearby aspirated thermocouples, for various tests in which the upper layer temperatures ranged from 400 °C (750 °F) to 800 °C (1500 °F). Intermediate temperatures were estimated based on linear interpolation between the higher and lower temperature results. Contributions to the uncertainty associated with radiative exchange are listed as U_r in Table 4-1. The component expanded uncertainties were used to compute the combined expanded uncertainty for a bare bead TC as listed in Table 4-2. The largest contributor to the overall uncertainty at high temperatures was the uncertainty in the aspirated thermocouple measurement, while at low temperatures the contribution of uncertainty in the radiative exchange was relatively more important.

In the lower layer of compartment fires with a smoky, high-opacity upper layer, radiative gain due to flux from the hot upper layer may lead to erroneously high thermocouple readings. This is not considered a significant problem for the model evaluation considered here, as the lower layer information is used only to determine the hot gas layer (HGL) depth. It is assumed that the uncertainty in the layer depth calculation is not significantly impacted by erroneously high lower layer TC readings, since the layer calculation looks for locations of temperature difference, rather than the value of that difference. A larger contributor to the uncertainty of the layer depth is the physical distance between thermocouples, which is the spatial resolution of the measurement. Consideration of the algorithm used to determine the HGL depth suggests that the uncertainty will be approximately one-half the distance between thermocouples at the location of the layer interface.

Table 4-3 summarizes the estimates of the relative expanded measurement uncertainties, U_e, associated with the HGL layer depth and temperature rise for the experiments considered in this report. For the HGL depth, the distance between thermocouples differed for each of the tests, varying from 0.1 m (4 in) to 0.3 m (12 in). Repeatability of the depth determination was investigated for BE #3 by examining the results for the repeat tests. The difference in the calculated HGL depth between the repeat measurements was about 3 %, on average. It was assumed that the repeatability in the other tests was similar to that determined in BE #3. Measurement repeatability was considered in the determination of U_e. The HGL depths varied from about 1 m (40 in) to 3 m (120 in) for all of the experiments considered here, and the relative expanded uncertainties in the values of the HGL depth varied from about 6 % to 23 % as seen in Table 4-3. The value of U_e does not accurately account for radiative exchange in NBS Test

100A, in which natural gas was the fuel. Treating the HGL in this case, as optically thick is inappropriate, and the value of U_e is likely small.

Ceiling jet measurements were conducted in BE #3 and the FM/SNL tests, in which the temperatures were measured using bare bead and aspirated thermocouples, respectively, and temperatures in the plume were conducted in BE #2 and the FM/SNL tests, in which the temperatures were measured using bare bead and aspirated thermocouples, respectively. Because the ceiling jet is located high in the hot smoky upper layer, radiative exchange effects on thermocouples should be minimal and the results are treated in the same way as the bare bead thermocouples in the upper layer.

Table 4-1: Expanded Measurement Uncertainty of a Bare Bead Thermocouple in the Hot Smoky Upper Layer of a Compartment Fire

Gas Temperature °C (°F)	U_w °C (°F)	U_r °C (°F)	U_a °C (°F)	U_e, Combined Expanded Uncertainty °C (°F)
0 (32)	2 (4)	0 (0)	2 (4)	3 (5)
60 (140)	2 (4)	5	3 (5)	6 (11)
120 (250)	2 (4)	6 (11)*	4 (7)	8 (14)
150 (300)	2 (4)	6 (11)*	5 (9)	8 (14)
300 (570)	2 (4)	9 (16)*	12 (22)	15 (27)
500 (930)	4 (7)	12 (22)	20 (36)	24 (43)
800 (1500)	6 (11)	12 (22)	32 (58)	35 (63)
* based on linear interpolation between the higher and lower temperature results.				

Repeatability of the ceiling jet temperatures was investigated for BE #3 by examining the results of the repeat tests. The difference between the repeat measurements was about 8 %, on average. The difference in the repeatability of the FM/SNL tests was assumed to be small, since radiative exchange effects were negligible with the use of aspirated thermocouples. The values of U_e for the ceiling jet varied from 4 % to 12 % as seen in Table 4-4 for the two test series considered here. Assessment of the uncertainty of the plume temperature measurements is more problematic. In this case, the bare bead thermocouple results are treated in the same manner as the bare bead thermocouple results for measurements in an upper layer. The repeatability of the BE #2 measurements was assumed to equal 8 %, the same as the ceiling jet measurements in BE #3. Still, the value of U_e is probably too small in the lower part of the plume for BE #2, which was not in a well-developed smoky upper layer. The values of U_e for the plume varied from 4 % to 11 % as seen in Table 4-5 for the two tests considered here.

Table 4-2: The Relative Expanded Uncertainties (U_e) Associated with the Measured HGL Depth and Temperature Rise

Series	U_e (%)	
	HGL Depth	**HGL Temperature Rise**
NBS	6	6 *
FM/SNL	23	10
BE #2	8	9
BE #3	6	6
BE #4	22	6
BE #5	9	7
* value of U_e does not accurately account for radiative exchange in Test 100A, in which natural gas was the fuel; its value is likely small; see text.		

Table 4-3: The Relative Expanded Uncertainties (U_e) Associated with the Measured Ceiling Jet Temperature Rise

Series	U_e (%)
	Ceiling Jet Temperature Rise
BE #3	12
FM/SNL	4

Table 4-4: The Relative Expanded Uncertainties (U_e) Associated with the Measured Plume Temperature Rise

Series	U_e (%)
	Plume Temperature Rise (°C)
BE #2 upper	9
BE #2 lower	11 *
FM/SNL	4
* the value of U_e is too small in the lower part of the plume in BE #2, which was not in a well-developed smoky upper layer.	

4.2 Gas Species Volume Fraction

The volume fractions of the combustion products CO and CO_2 were measured using gas sampling in conjunction with non-dispersive infrared analyzers, while the O_2 volume fraction was typically measured using a paramagnetic analyzer. Gases were extracted through stainless steel or other types of lines and were pumped from the compartment and passed through the analyzers. For several reasons, water in the sample was typically filtered, so the reported results are denoted as "dry" and comparison with model results must be corrected. Analyzers were calibrated through the use of standard gas mixtures, with low relative uncertainties. Problems with the technique may involve instrument drift, analyzer response, incomplete and partial drying of sample gases, or in the case when drying is not used, undetermined amounts of water vapor in the oxygen cell resulting in inaccurate readings.

Measurements of gas species volume fractions are considered for two of the experiments, namely BE #3 and BE #4. The species were measured in the upper and lower layer at a single location in BE #3. The relative expanded uncertainty in the measured values in BE #3 were about 3 % for both the oxygen depletion and the CO_2 measurements. The largest contributor to the uncertainty was uncertainty in the composition of the calibration gas and the possibility of an undetermined amount of water vapor in the sample. Repeatability of the gas measurements was investigated for BE #3 by examining the results for the repeat tests. The difference between the repeat measurements was about 2 %, on average, for both the oxygen depletion and the carbon dioxide measurements. Combining the uncertainties, the relative expanded uncertainty was typically 4 % for both, the CO_2 gain and the O_2 depletion, measurements. It was assumed that the uncertainty in BE #5 was similar to that determined in BE #3.

Table 4-5: Summary of the Relative Expanded Uncertainties Associated with the Oxygen and Carbon Dioxide Concentrations

Series	U_e (%)		
	HGL CO_2 Concentration	**HGL O_2 Concentration Decrease**	**LGL O_2 Concentration Decrease**
BE #3	4	4	4
BE #5	4	4	4

4.3 Smoke Concentration

The mass based smoke concentration was measured in one of the experiments, namely BE #3. In that experiment, smoke was measured using laser transmission at 632.8 nm. The reported mass concentration of smoke, M_s, was computed using the following expression:

$$M_s = \frac{\ln(I_0 / I)}{\phi_s L} \tag{4.1}$$

where L is the path length, I and I_o are the laser signal and reference signal and ϕ_s is the specific extinction coefficient, which has a nearly universal value of 8.7 $m^2/g \pm 5$ % for hydrocarbons [Ref. 32]. Other uncertainties in the measurement were due to errors in the path length, L, and the light attenuation, I_0 / I. In BE #3, Ref. 5 reported the expanded uncertainty of the M_s measurement as 18 %, with the dominant contribution to the uncertainty coming from drift in the laser measurement. Repeatability of the smoke measurement was investigated for BE #3 by examining the results for the repeat tests. The mean difference between the measurements was about 21 %. Therefore, a combined expanded experimental uncertainty of 28 % is suggested.

Table 4-6: The Relative Expanded Uncertainties (U_e) Associated with the Measured Smoke Concentration and the Compartment Pressure

Series	U_e (%)	
	Smoke Concentration	**Pressure**
BE #3	28	27

4.4 Pressure

The compartment pressure was only measured in one of the experiments, namely BE #3. The uncertainty in pressure measurements is typically small, but depends on the sensor type and its calibration. In BE #3, the differential pressure gauge used was temperature compensated, highly-linear, and very stable. A conservative estimate of the expanded measurement uncertainty led to a value of 1 %. Repeatability of the pressure measurement was investigated for BE #3 by examining the results for the repeat tests. The average difference between the repeat measurements was about 27 %. Compartment leakage is a likely explanation for the large difference between repeat tests. An expanded uncertainty value of 27 % is suggested in Table 4-7.

4.5 Heat Flux

Measurements of the heat flux are considered for three of the experiments, namely BE #3, BE #4, and BE #5. Heat flux gauges were used to measure the transport of radiant energy or the combination of radiation and convection. Several types of gauges were used and different types of instrumentation and procedures were used to calibrate the gauges. In BE #3, four types of gauges were used including those that measured total heat flux, or just radiative heat flux. In BE #4 and BE #5, total heat flux gauges were used.

The uncertainty associated with a heat flux measurement depends on many factors including gauge characteristics, the calibration conditions and accuracy, as well as the incident flux modes (convective, radiative, conductive) and their magnitudes in the actual measurement situation [Ref. 33]. Ref. [34] performed two rounds of an international round-robin test of heat flux gauges in which five fire laboratories performed independent calibrations of two sets of Gardon and Schmidt-Boelter total heat flux gauges. The results showed that the calibrations agreed to within about 5 %. Typically, the reported expanded uncertainties of heat flux gauges varies from about 5 % to 10 %, with the measurement uncertainty typically dominated by uncertainty in the calibration and repeatability of the measurement. Ref. [33] suggests that much higher values may be more realistic, depending on the exact nature of the fire conditions and the type of gauge. Repeatability of the various heat flux measurements in BE #3 was determined by examining measurements by the same instruments for different pairs of repeat tests. The difference between the measurements was about 7 %, on average, for both the radiative flux measurements and the total flux measurements. In this report, an expanded uncertainty value of about 10 % is suggested based on the BE #3 measurement repeatability and calibration uncertainties. It is assumed that the measurement uncertainty in BE #4 and BE #5 was similar to BE #3 as listed in Table 4-8.

Table 4-7: Summary of the Relative Expanded Uncertainties Associated with the Measured Target Heat Flux and Target Temperatures

Series	U_e (%)	
	Total Heat Flux to Targets	**Rise in Target Surface Temperature**
BE #3	10	1 – 7
BE #4	10	1 - 2
BE #5	10	4

4.6 Surface/Target Temperature

Bare bead thermocouples were used to measure the temperature of targets and compartment surfaces. A typical method is to "peen" the thermocouple into surface, that is, to bend and effectively spring-load the metal thermocouple until physical contact with the surface or target occurs. Heating of the thermocouple can cause it to undergo a shape change, which can cause a "peened" thermocouple to have poor physical contact with a surface. Another method pulls on the leads of a thermocouple with a small gravity load, forcing it to make physical surface.

The inherent expanded uncertainty associated with a type K thermocouple is approximately 2 °C (4 °F) for temperatures below 200 °C (390 °F) [Ref. 31]. Repeatability of the surface and cable temperature measurements was investigated in BE #3 by examining the measurements of the same instruments for different repeat tests. The difference between the measurements was about 8 % and 7 %, on average, for the cable and wall surface measurements, respectively. Combining the inherent thermocouple uncertainty and the repeatability yields uncertainty on the order of 10 % for the thermocouple surface measurements. It is assumed that the measurement uncertainty in BE #4 and BE #5 was similar to BE #3.

Table 4-8: Summary of the Relative Expanded Uncertainties Associated with the Surface Heat Flux and Temperatures

Series	U_e (%)	
	Total Heat Flux	**Rise in Surface Temperature**
BE #3	10	10
BE #4	10	10
BE #5	10	10

4.7 Summary

In general, measurement uncertainty depends on many issues, including the exact type of instrumentation, the experimental procedure, and the details of the measurement scenario. Because uncertainty was not documented for most of the experiments considered in this report, engineering judgment was used to provide estimates of measurement uncertainty for each of the parameters of interest. This information on *measurement uncertainty* is combined with *the model input uncertainty* in Chapter 6 to provide a basis for the evaluation of the fire models, as described in Volumes 2-6 of this report.

5
SENSITIVITY OF MODEL RESULTS TO UNCERTAINTY IN MEASURED INPUT PARAMETERS

In this chapter, the sensitivity of model results to uncertainty in measured input parameters, referred to here as the *model input uncertainty* (U_m), is quantified. There are a number of ways that this could be achieved. A sensitivity analysis for the models could have been performed by running many calculations and determining the variation of a calculated output parameter as a function of the change in one or more input parameters. This is a brute force approach, which provides relevant information, but is labor intensive and does not necessarily offer physical insight. In addition, such an approach would be model specific. Rather than a brute-force method, the approach presented here is based on correlations available in the fire literature.

For each parameter of interest, a simple analytic description of the sensitivity of that parameter to the fire HRR is given. For example, the nature of the hot gas layer (HGL) is largely a function of the fire size, and the uncertainty in the HRR measurement for the various experiments ranged from 15 % to 25 %. The dependence has been quantified based on results documented in the technical literature, in which simple analytical relationships or *correlations* have been developed from measurements made in many compartment fire experiments performed over several decades. Using the empirical correlations, it is possible to estimate how the uncertainty in the specified HRR influences the various parameters of interest. The magnitude of this uncertainty (U_m) plays an important role in the evaluation of model accuracy through consideration of Eq. 1.4 in Chapter 1. The remainder of this chapter discusses the sensitivity of model output parameters to the model input parameters.

5.1 Hot Gas Layer and Ceiling Jet Temperatures

According to an empirical correlation by McCaffrey, Quintiere and Harkleroad (MQH) [Ref. 35], the HGL temperature is proportional to the HRR raised to the two-thirds power:

$$T_g - T_\infty = 6.85 \left(\frac{\dot{Q}^2}{A_0 \sqrt{H_0} h_k A_T} \right)^{1/3} \tag{5.1}$$

where $\dot{Q}$ is the heat release rate in kW, A_0 is the area of the opening, H_0 is the height of the opening, $h_k = k/\delta_w$ is the heat transfer coefficient, k is the thermal conductivity (kW/m/K), δ_w is the wall thickness (m), and A_T is the total compartment surface area (m^2). Although the MQH correlation has limitations, it encapsulates a set of observations that give insight into trends associated with HGL temperature.

The uncertainty in the HRR measurement for the various experiments ranged from 15 % to 25 %. The uncertainty in the HGL temperature *prediction* varies, therefore, by 2/3 from the uncertainty in the HRR *measurement*.

According to the empirical ceiling jet correlations by Alpert [Ref. 36], the temperature within the ceiling jet is also proportional to the HRR raised to the two-thirds power, thus the same sensitivity to the HRR should apply for the ceiling jet temperature as for HGL temperature.

5.2 Hot Gas Layer Depth

The location of the HGL is relatively insensitive to the HRR of the fire. According to the correlation of Heskestad and Delichatsios [Ref. 37], the layer height, z, is given by the function:

$$\frac{z}{H} = 1.11 - 0.28 \ln\left(\frac{t\,\dot{Q}^{1/3}\,H^{-4/3}}{A/H^2} \right) \tag{5.2}$$

The rate of change of the height with time, according to this expression, is not a function of the HRR at all:

$$\frac{dz}{dt} = -\frac{0.28\,H}{t} \tag{5.3}$$

where H is the ceiling height. This equation shows that the rate of change with time becomes small for large values of t. Empirical correlations relating the sensitivity of the layer height to the HRR were not found in the literature. It should be noted that in fire scenarios with open doors or windows, the gas layer height is largely affected by the position of the soffit. The dependence of the HGL depth to the HRR was presumed to be weak. Yet, experimental observation suggests that the depth is a function of the door opening size and the relative size of the fire.

To confirm the weak dependence of the HGL depth to the HRR, a sensitivity analysis was conducted using CFAST for Test 3 of BE #3. The HGL depth in CFAST is not a result of a simple correlation from the fire literature, but is a product of the solution of the energy and mass conservation equations. The CFAST results showed that there was about a ±2 % change in the HGL depth for a ±15 % change in the HRR. A 25 % uncertainty in the HRR would be expected to yield a 3 % uncertainty in the depth. The dependence of the HGL depth on the HRR is weak, but non-zero. The reasons for this likely involve a balance between the increasing HGL temperature and decreasing density and the balance of flows in and out of the compartment.

5.3 Plume Temperature

The plume temperature is mainly a function of the HRR. According to McCaffrey's correlation of fire plume temperature and velocity [Ref. 38], the centerline temperature at heights between 1.3 D^* and 3.3 D^* is proportional to the HRR to the two-fifths power, whereas at heights greater than 3.3 D^*, the temperature rise is proportional to the two-thirds power, just like the HGL relationship. A similar argument can be made for the sensitivity of the fire plume temperature rise to HRR as that for the HGL temperature rise.

5.4 Flame Height

According to the empirical correlation by Heskestad [Refs.38, 39], flame height, L, is related to the HRR and the "diameter" of the fire via the expression:

$$\frac{L}{D} = 3.7\,\dot{Q}^{*2/5} - 1.02 \quad ; \quad \dot{Q}^{*} = \frac{\dot{Q}}{\rho_\infty c_p T_\infty \sqrt{gD}D^2} \tag{5.4}$$

which is valid for values of $\dot{Q}^{*}$, such that $0.12 < \dot{Q}^{*} < 1.2 \cdot 10^{4}$. Evaluating the constants, Heskestad [Ref. 38] gives an expression that is approximately valid for most types of hydrocarbon pool fires:

$$L = -1.02\,D + 0.235\,\dot{Q}^{2/5} \tag{5.5}$$

From this relationship, the sensitivity of the flame height to the HRR can be inferred. Considering a small change in L, denoted as δL, leads to:

$$\frac{\delta L}{L} = \frac{2}{5}(1 + 1.02\,D/L)\,\frac{\delta \dot{Q}}{\dot{Q}} \tag{5.6}$$

For the experiments considered in this report, a representative relation between D and L is $D \sim \frac{1}{3} L$, so Eq. 5.6 is approximately:

$$\frac{\delta L}{L} \sim \tfrac{1}{2}\,\frac{\delta \dot{Q}}{\dot{Q}} \tag{5.7}$$

and an uncertainty of 15 % or 25 % in the HRR, leads to an uncertainty of about 8 % or 13 %, respectively, in the flame height.

5.5 Gas Concentration

Most fire models assume that combustion product gases, once generated in the fire, are passively transported throughout the compartment. The major products of combustion, like carbon dioxide and water vapor, plus the major reactant, oxygen, are generated, or consumed, in direct proportion to the burning rate, which is directly proportional to the HRR. The mass fraction of any species in the HGL is related to its yield times the mass entrained into the upper layer [Ref. 37]:

$$Y_i = \frac{y_i \dot{m}}{\dot{m}_e} = \frac{y_i \dot{Q}}{\chi_a H_c \dot{m}_e} \tag{5.8}$$

where $\dot{m}$ is the fuel mass burning rate (equal to $\frac{\dot{Q}}{\dot{m}\chi_a H_c}$), and $\dot{m}_e$ is the mass entrained into the upper layer, which is approximately equal to the air entrained into the upper layer [Ref. 37]):

$$\dot{m}_e = 0.0059\,\dot{Q}\;Z/L \tag{5.9}$$

where Z is a vertical location above the surface of the fire below which air entrainment occurs and L is the flame height (for a fire burning in the open). Here, Z is taken as the location of the HGL, which can be approximated as the position the soffitt in a compartment fire with natural ventilation, and Z is always less than or equal to L by definition.

$$Y_i = \frac{y_i L}{0.0059 Z \chi_a H_c} \tag{5.10}$$

From this relationship, the sensitivity of Y_i to the HRR can be inferred. The terms other than L in the above equation represent parameters that are assumed to be constants for the ventilated compartment fire experiments that represent most of the experiments considered in this report. In fact, the combustion efficiency and the values of y_i are functions of fire conditions in the compartment, particularly when the fire is underventilated. Considering a small change in Y_i, denoted as δY_i, leads to:

$$\frac{\delta Y_i}{Y_i} = \frac{\delta L}{L} \approx \tfrac{1}{2} \frac{\delta \dot{Q}}{\dot{Q}} \tag{5.11}$$

and from Eq. 5.11, the uncertainty in the change of a gas species in the HGL is can be related to the uncertainty in $\dot{Q}$. An uncertainty of 15 % in the HRR, leads to a change of about 8 % in the CO_2 and O_2 volume fractions.

5.6 Smoke Concentration

Smoke, or soot, is a product of incomplete combustion. Smoke particulate is not a gas, but a complex solid whose form and concentration depend on the type of fuel and the ventilation conditions within the compartment. Once formed, it is transported with other combustion products. A simple assumption used in many zone and field fire models is that smoke is transported in the same way as gas products. The soot generation rate or soot *yield per unit fuel mass,* y_s, is difficult to predict and the fire models are subject to error due to uncertainty in the prescribed soot yield. The soot yield for BE #3 was reported as 1.5 ± 18 % for heptane [Ref.5]. This uncertainty, however, is a measurement uncertainty and omits changes in chemistry that may occur, for example, during an underventilated compartment fire. In the upper layer of a compartment fire, the mass of soot per unit volume, M_s, is equal to the product of the mass fraction of soot (Y_s) and the density (ρ) of the HGL:

$$M_s = \rho Y_s \tag{5.12}$$

Considering a small change in M_s, denoted as δM_s, and using the chain rule:

$$\frac{\delta M_s}{M_s} = \frac{\delta \rho}{\rho} + \frac{\delta Y_s}{Y_s} \tag{5.13}$$

The relation between $\frac{\delta Y_i}{Y_i}$ and $\frac{\delta \dot{Q}}{\dot{Q}}$ is given by Eq. 5.11. A term for the uncertainty in the soot yield ($\frac{\delta y_s}{y_s}$), which arises from Eq. 5.10 must also be considered. The relation between the change in the density and the HRR is determined from the ideal gas law,

$$\frac{\delta \rho}{\rho} \sim \frac{\delta (1/T)}{(1/T)} = - \frac{\delta T}{T} \tag{5.14}$$

From Eq. 5.1, $\delta T \approx 2/3\ \dot{Q}^{-1/3}\ \delta\dot{Q}$, so

$$\frac{\delta T}{T} = 2/3\ (1-\frac{T_\infty}{T_g})\ \frac{\delta\dot{Q}}{\dot{Q}} \tag{5.15}$$

Substituting Eqs. 5.11, 5.14, and 5.15 into 5.13 yields:

$$\frac{\delta M_s}{M_s} = [\ 2/3\ \frac{T_\infty}{T_g} - 1/6]\ \frac{\delta\dot{Q}}{\dot{Q}} \quad + \frac{\delta y_s}{y_s} \tag{5.16}$$

An uncertainty in $\dot{Q}$ leads to an uncertainty in M_s that is dependent on the ratio of the (absolute) ambient temperature to the gas temperature. For T_g equal to 200 ^{o}C (473 K), an uncertainty of 15 % in $\dot{Q}$ leads to an uncertainty of about 4 %, in M_s. In this example, a value of 200 ^{o}C was selected for T_g, because it represents a typical HGL temperature during the BE #3 tests. The uncertainty due to heat release rate is therefore small, and the dominant contributor is uncertainty in the soot yield.

5.7 Pressure

In a closed compartment, the average pressure, p_0, is governed by the equation

$$\frac{dp_0}{dt} = \frac{\gamma-1}{V}\left(\dot{Q}-\dot{Q}_{\text{loss}}\right) - \frac{\gamma\ p_0}{\text{V}}\left(\dot{V}_{\text{out}} - \dot{V}_{\text{in}} + \dot{V}_{\text{leak}}\right) \tag{5.17}$$

Here, γ is the ratio of specific heats (about 1.4), V is the volume of the enclosure, $\dot{Q}_{\text{net}} = \dot{Q} - \dot{Q}_{\text{loss}}$ is the net rate of energy heating up the gases in the compartment, and the $\dot{V}$ terms are the volume flow out of the compartment due to the exhaust, the volume flow into the compartment due to a fan, and the leakage, respectively. The volume flow rate due to leakage is given by:

$$\dot{V}_{\text{leak}} = A_{\text{leak}}\sqrt{\frac{2\,(p_0 - p_\infty)}{\rho_\infty}} \tag{5.18}$$

where A is the leakage area. The maximum compartment pressure is achieved when the pressure rise in Eq. 5.17 is set to zero. Rearranging terms, an estimate for the maximum pressure in the compartment can be made as follows:

$$(p_0 - p_\infty)_{\max} \cong \frac{\rho_\infty}{2}\left(\frac{(\gamma-1)\,\dot{Q}_{\text{net}} - \gamma\ p_\infty \dot{V}_{\text{vent}}}{A_{\text{leak}}\ \gamma\ p_\infty}\right)^2 \tag{5.19}$$

The term $\dot{V}_{\text{vent}}$ is the net ventilation volume flow. The expression for the maximum pressure can be used to estimate the uncertainty in the model prediction to changes in the measured HRR, net ventilation volume flow, and leakage area.

The compartment pressure was considered using data from BE #3 only. The uncertainty in A_{leak} for the open-door experiments was very small, but for the closed door tests, an uncertainty of

10 % to 15 % is expected [Ref. 5]. The uncertainty in $\dot{Q}_{net}$ is dominated by uncertainty in $\dot{Q}$. In the absence of forced ventilation, an uncertainty of 15 % in the HRR and leads to an uncertainty of 30 % in pressure. For the closed door tests with ventilation, the uncertainty in $\dot{V}_{\text{vent}}$ is difficult to characterize because the mechanical flows were generally not well characterized in the experiments. It is estimated that an uncertainty of 30 % is not unreasonable, leading to an uncertainty of about 75 % in pressure for the closed-door vented condition.

5.8 Heat Flux

The radiative heat flux onto surfaces in the upper layer is nearly equal to $\varepsilon\sigma T^4$ where ε is the effective emissivity of the upper layer, $\sigma = 5.67 \times 10^{11}$ kW/m^2/K^4, and T is the upper layer gas temperature in Kelvin. Considering a small change in the flux, $\dot{q}''$, denoted as $\delta\dot{q}''$, leads to:

$$\delta\dot{q}'' = 4\, T^3\, \delta T \tag{5.20}$$

Considering Eq. 5.20, the fractional change in $\dot{q}''$, $(\frac{\delta\dot{q}''}{\dot{q}''})$ is equal to:

$$\frac{\delta\dot{q}''}{\dot{q}''} \approx 8/3\ \frac{\delta\dot{Q}}{\dot{Q}}\,(1-\frac{T_\infty}{T_g}) \tag{5.21}$$

so that, an uncertainty of 15 % in the HRR, leads to an uncertainty of about 15 % in $\dot{q}''$ for T_g equal to 200 ^{o}C (473 K), typical of the HGL temperature during the BE #3 tests. For BE #4, the temperature was much higher (~1000 K), and the 25 % uncertainty in the HRR leads to an uncertainty of about 50 % in $\dot{q}''$.

5.9 Wall/Target Surface Temperature

The surface temperature of the walls and targets is a function of the heat flux, the thermophysical and optical properties of the material, and its temperature. A simplistic approach to uncertainty considers a well-insulated wall or ceiling surface in the optically thick HGL of a compartment fire. After steady state is reached, uncertainty in the HRR leads to uncertainty in the HGL temperature, which translates into uncertainty of the surface or target temperature. An uncertainty in the HRR of 15 % corresponds to uncertainties of 10 % in the upper layer and wall temperatures.

5.10 Summary

The empirical correlations described in this chapter provide recipes to calculate the uncertainty in the model outputs resulting directly from the uncertainty in key input parameters. For example, a two-thirds power dependence of HGL temperature on the HRR means that the uncertainty in the predicted HGL temperature is about two-thirds the uncertainty in the measured HRR. This uncertainty does not include the measurement uncertainty. For example, it does not include whatever error is associated with the thermocouple itself. For many of the measured quantities under consideration, the *model input uncertainty* is greater than the *measurement uncertainty* as discussed in the next chapter.

Table 5-1 lists the measured quantities, along with the parameters that most influence them. The last column in the table lists the uncertainties in the given quantity based on the combined uncertainty of the key parameters. For illustrative purposes, the propagated model input uncertainty results, U_m, shown in the Table is based on an expanded (2σ) uncertainty of 15 % for the HRR, although this value actually varied from 15 % to 25 % for the six test series (see Table 2-1). The resulting values of the propagated uncertainty for the various parameters should be regarded as the expanded value.

Table 5-1: Summary of the model sensitivity, U_m, to uncertainty in the HRR

Quantity	**Input Parameter**	**Power Dependence**	**Expanded Uncertainty, U_m (%)**
HGL Temperature, T_g	$\dot{Q}$	$2/3$	10
HGL Depth, z	$\dot{Q}, A, H$	Eq (5.3)	2
Ceiling Jet Temperature	$\dot{Q}$	$2/3$	10
Plume Temperature	$\dot{Q}$	$2/5 \quad 1.3 < z/D^* < 3.3$ $2/3 \quad 3.3 < z/D^*$	6 10
Flame Height	$\dot{Q}$, D	½	8
Gas Concentrations	$\dot{Q}$	½	8
Smoke Concentration	$\dot{Q}$, y_s	Eq (5.16), 1	18 **
Pressure	$\dot{Q}$, A_{leak}, $\dot{V}_{vent}$	2, 2, 2	30 (no forced ventilation) 75 (with ventilation)
Heat Flux, $\dot{q}''$	$\dot{Q}$	Eq (5.21)	15 **
Surface/Target Temperature	$\dot{Q}$	2/3	10

* actual uncertainty in the HRR varied from 15 % to 25 % among the experiments, and there was also some variation among the tests for a single experimental series (see Table 2-1 and text).

** for $T_g \approx 200\ ^{o}C$.

6
REPRESENTATIVE UNCERTAINTIES

6.1 Summary of the Estimated Measurement Uncertainty and Subsequent Model Input Uncertainties

A summary of the estimated measurement and model input uncertainties are presented in this section. The uncertainties for each of the parameters of interest in each of the experimental series are listed below in Tables 6-1 to 6-7. Each table contains information on the expanded (2σ) relative measurement uncertainty (U_e), the expanded (2σ) relative model input uncertainty associated with model input uncertainty (U_m), and the combined relative expanded (2σ) uncertainty (U_c), defined in Eq. 1.3 as: $U_c = U_\varepsilon = (U_e^{\,2} + U_m^{\,2})^{1/2}$. The values of U_e are taken from Tables 3-2 to 3-9. The values of the HRR uncertainty for each experiment are taken from Table 2-1.

Table 6-1: Summary of the Relative Expanded Uncertainties Associated with the HGL Layer Depth and Temperature Rise

Series	HGL Depth			HGL Temperature Rise		
	U_e (%)	U_m (%)	U_c (%)	U_e (%)	U_m (%)	U_c (%)
NBS	6	2	6	6 *	10	12
FM/SNL	23	2	23	10	13	16
BE #2	8	2	8	9	10	13
BE #3	6	2	6	6	11	12
BE #4	22	2	22	6	17	18
BE #5	9	2	9	7	10	12

* the value of U_e does not accurately account for radiative exchange in Test 100A, in which natural gas was the fuel; its value is likely small (see text in Section 3.2.3).

Table 6-2: Summary of the Relative Expanded Uncertainties Associated with Ceiling Jet Temperatures

Series	Ceiling Jet Temperature Rise		
	U_e (%)	U_m (%)	U_c (%)
BE #3	12	11	16
FM/SNL	4	13	14

Table 6-3: Summary of the Relative Expanded Uncertainties Associated with Plume Temperatures

Series	Plume Temperature Rise (°C)		
	U_e (%)	U_m (%)	U_c (%)
BE #2 upper	9	10	14
BE #2 lower	11 *	10	15
FM/SNL	4	13	14
* the value of U_e does not accurately account for radiative exchange; its value is likely small (see text).			

Table 6-4: Summary of the Relative Expanded Uncertainties Associated with Oxygen and Carbon Dioxide

Series	HGL CO_2 Concentration			HGL O_2 Concentration Decrease			LGL O_2 Concentration Decrease		
	U_e (%)	U_m (%)	U_c (%)	U_e (%)	U_m (%)	U_c (%)	U_e (%)	U_m (%)	U_c (%)
BE #3	4	8	9	4	8	9	4	8	9
BE #5	4	8	9	4	8	9	4	8	9

Table 6-5: Summary of the Relative Expanded Uncertainties Associated with the Smoke Concentration and the Compartment Pressure

Series	Smoke Concentration			Pressure		
	U_e (%)	U_m (%)	U_c (%)	U_e (%)	U_m (%)	U_c (%)
BE #3	28	20	33	27	30 (no vent) 75 (vent)	40 (no vent) 80 (vent

Table 6-6: Summary of the Relative Expanded Uncertainties Associated with the Target Heat Flux and Target Temperatures

Series	Total Heat Flux to Targets			Rise in Target Surface Temperature		
	U_e (%)	U_m (%)	U_c (%)	U_e (%)	U_m (%)	U_c (%)
BE #3	10	16	19	10	11	14
BE #4	10	47	48	10	13	16
BE #5	10	13	17	10	10	14

Table 6-7: Summary of the Relative Expanded Uncertainties Associated with the Surface Heat Flux and Surface Temperatures

Series	Total Heat Flux			Rise in Surface Temperature		
	U_e (%)	U_m (%)	U_c (%)	U_e (%)	U_m (%)	U_c (%)
BE #3	10	16	19	10	11	14
BE #4	10	47	48	10	13	16
BE #5	10	13	17	10	10	14

6.2 Representative Uncertainties

Using engineering judgment, a weighted expanded combined uncertainty, U_{cw}, representative of the uncertainty for each of the parameters was estimated:

$$U_{cw} = \frac{1}{\sum_{i=1}^{6} n_i} \sum_{i=1}^{6} U_c n_i \qquad (5.1)$$

where the weighted average used the combined expanded uncertainties (U_c listed in Tables 6-1 through 6-6), and was based on the sum of the number of tests (n_i) (see Table 1-1) for the parameters of interest for each of the six test series (i). A weighted average based on the number of experimental tests was used rather than some other weighting approach, because the model evaluation considered each of the 26 tests as independent trials (see Chapter 6, Volumes 2 to 6). The number of experiments (and the associated number of tests), and these varied for each parameter. The weighted expanded combined uncertainty, U_{cw}, and the total number of tests ($\sum_{i=1}^{6} n_i$) for each of the parameters is shown in Table 6-8. Fifteen of the tests were from BE #3, and in this sense, the results from BE #3 strongly influenced the results.

Table 6-8: The weighted combined expanded uncertainty, U_{cw}, determined from Eq. 5.1 and Tables 6-1 through 6-7

Quantity	Number of Tests	Weighted Expanded Combined Uncertainty, U_{cw} (%)
HGL Temperature rise, T_g	26	13
HGL Depth, z	26	9
Ceiling Jet Temperature	18	16
Plume Temperature	6	14

Quantity	Number of Tests	Weighted Expanded Combined Uncertainty, U_{cw} (%)
Gas Concentrations	16	9
Smoke Concentration	15	33
Pressure	15	40 (no forced ventilation) 80 (with forced ventilation)
Heat Flux, $\dot{q}''$	17	20
Surface/Target Temperature	17	14

6.3 Conclusions

In this evaluation, fire experiments are used as a way of establishing confidence in model predictions. As part of the evaluation considered in this report series, the effect of experimental uncertainty on both models and measurements is considered. A literature search was conducted to select experiments that would allow evaluation of key aspects of fire models. In general, the report of experiments did not adequately address measurement uncertainty.

There may be many reasons for this, but an important reason is that the expense of performing a comprehensive uncertainty analysis is often larger than the cost of the measurement itself. Without such analysis, however, the fire measurements are unlikely to experience improvement in accuracy. Experimental design and execution must carefully address measurement uncertainty, and in particular, attempt to reduce the uncertainty in key experimental parameters, most notably, the fire HRR. The ability to accurately and precisely measure HRR requires a significant institutional investment, as a facility must be well-instrumented, its performance characterized, and the uncertainties analyzed and documented.

In this study, measurement uncertainty was estimated for the experiments of interest using engineering judgment. The importance of the uncertainty in the HRR was emphasized in this study, because this parameter drives the thermal environment in the model calculation results, and the calculation results are sensitive to the uncertainty of this parameter. Quantifying the uncertainty in the HRR provides a basis for understanding model sensitivity to this parameter, taken here as a representation of model input uncertainty. To date, there have not been many fire model verification and validation studies based on ASTM 1355. There have been few that have tried to document experimental uncertainty as part of the analysis. The uncertainty in model output was assessed through consideration of the uncertainty in measured quantities that are used as input for the models. Both measurement uncertainty and model input uncertainty are found to be important and both contribute to the combined uncertainty. The information from this volume is used as a basis for the model evaluation as discussed in Volumes 2-6 of this report series.

7
REFERENCES

1. ASTM Standard Guide for Evaluating the Predictive Capability of Deterministic Fire Models, ASTM E1355-05, American Society for Testing and Materials, West Conshohocken, PA 2005.
2. Nowlen, S.P., Enclosure Environment Characterization Testing for the Base line Validation of Computer Fire Simulation Codes, NUREG/CR-4681, SAND86-1296, Sandia National Laboratories, Albuquerque, NM, March 1987.
3. Peacock, R. D.; Davis, S.; Lee, B. T. Experimental Data Set for the Accuracy Assessment of Room Fire Model, National Bureau of Standards, Report NBSIR 88-3752; 120 p., April 1988.
4. Hostikka, S., Kokkala, M., Vaari, J., "Experimental Study of the Localized Room Fires," NFDC2 Test Series, VTT Research Notes 2104, 2001.
5. Hamins, A., Maranghides, A., Johnsson, E., Donnelly, M., Yang, J., Mulholland, G., and Anleitner, R., *Report of Experimental Results for the International Fire Model Benchmarking and Validation Exercise #3*, NIST Special Publication 1013-1, National Institute of Standards and Technology, Gaithersburg, MD, 2005.
6. Klein-Heßling, W. and M.Röwenkamp, *Evaluation of Fire Models for Nuclear Power Plant Applications: Fuel Pool Fire inside a Compartment*. May 2005.
7. Hosser, D., Riese, O., and Klingenberg, M., *Performing of Recent Real Scale Cable Fire Experiments and Presentation of the Results in the Frame of the International Collaborative Fire Modeling Project ICFMP*, June 2004.
8. International Organization for Standardization (ISO), "Guide to the Expression of Uncertainty in Measurement," Geneva, Switzerland, 1993.
9. Taylor, B.N., and Kuyatt, C.E., *Guidelines for Evaluating and Expressing the Uncertainty of NIST Measurement Results*, National Institute of Standards and Technology (NIST) Technical Note 1297, 1994.
10. Hogg, R.V. and Tanis, E.A., Probability and Statistical Inference, 2nd Ed., MacMillan, 1983.
11. Bryant, R., Ohlemiller, T., Johnsson, E., Hamins, A., Grove, B., Guthrie, W.F., Maringhides, A., and Mulholland, G., *The NIST 3 Megawatt Quantitative Heat Release Rate Facility - Procedures and Guidance,* NIST Special Publication 1007, National Institute of Standards and Technology. Gaithersburg, MD, December 2003.
12. Axelsson, J., Andersson, P., Lonnermark, A., VanHees, P. and Wetterlund, I., *Uncertainties in Measuring Heat and Smoke Release Rates in the Room/Corner Test and the SBI*, SP Report 2001:04 SP Swedish National Testing and Research Institute, Boras, Sweden, (2001).

13. Enright, P.A., and Fleischmann, C.M., *Uncertainty of Heat Release Rate Calculation of the ISO5660-1 Cone Calorimeter Standard Test Method*, Fire Technology 35, 153-169 (1999).

14. Yeager, R.W., *Uncertainty Analysis of Energy-Release Rate Measurement for Room Fires,* J. Fire Sciences 4, 276-296 (1986).

15. Janssens, M.L., *Variability in Oxygen Consumption Calorimetry Tests*, (1427), American Society for Testing and Materials (ASTM), Dallas, TX, 147-162 (2002).

16. Tewarson, A., *Prediction of Fire Properties of Materials*, Part 1., National Bureau of Standards, NBS-GCR-86-521, December 1986.

17. Twearson, A., *Generation of Heat and and Chemical Compounds in Fires,* The SFPE Handbook of Fire Protection Engineering, 3rd Ed. (Section 3, Chap 4), National Fire Protection Association and The Society of Fire Protection Engineers, Quincy, MA, (Eds.: P. J. DiNenno, D. Drysdale, C. L. Beyler, and W. D. Walton, eds.), 2003.

18. Barbrauskas, V., Estimating Large Pool Fire Burning Rates, Fire Technology, 19, 251-261, 1983.

19. NUREG/CR-5384, A Summary of Nuclear Power Plant Fire Safety Research at Sandia National Laboratories, 1975–1987, December 1989.

20. Nowlen, S.P., *Enclosure Environment Characterization Testing for the Base line Validation of Computer Fire Simulation Codes*, NUREG/CR-4681, SAND86-1296, Sandia National Laboratories, Alburquerque, NM, March 1987.

21. Hamins, A., Maranghides, M., and Mulholland, G., The Global Combustion Behavior of 1 MW to 3 MW Hydrocarbon Spray Fires Burning in an Open Environment, National Institute of Standards and Technology. Gaithersburg, MD, Internal Report NISTIR 7013, June 2003.

22. Hamins, A., Klassen, M., Gore, J., and Kashiwagi, T., Estimate of Flame Radiance via a Single Location Measurement in Liquid Pool Fires, Combust. Flame, 86, 223-228 (1991).

23. Fire Modeling Code Comparison (TR-108875), Electric Power Research Institute (EPRI), Palo Alto CA.

24. Hostikka, S., VTT, Helsinki, Finland, personal communication, 2005.

25. Bundy, M., NIST, Gaithersburg, MD, personal communication, 2005.

26. Peacock, R.D., and Babrauskas, V., *Analysis of Large-Scale Fire Test Data,* Fire Safety Journal, 17, 387-414, 1991.

27. Blevins, L.G., *Behavior of Bare and Aspirated Thermocouples in Compartment Fires*, Proceedings of the 33rd National Heat Transfer Conference, Albuquerque, NM., August 15-17, 1999.

28. Pitts, W. M., Braun, E., Peacock, R. D., Mitler, H. E., Johnsson, E. L., Reneke, P. A., and Blevins, L. G., *Temperature Uncertainties for Bare-Bead and Aspirated Thermocouple Measurements in Fire Environments,* National Institute of Standards and Technology (NIST), Internal Report NISTIR 6242, October 1998.

29. Hamins, A., Maranghides, A., Johnsson, E., Donnelly, M., Yang, J., Mulholland, G., and Anleitner, R., *Report of Experimental Results for the International Fire Model Benchmarking*

and Validation Exercise #3, NIST Special Publication 1013-1, National Institute of Standards and Technology, Gaithersburg, MD, 2005.

30. Hamins, A., Maranghides, A., McGrattan, Ohlemiller, T., and Anleitner, R., Federal Building and Fire Safety Investigation of the World Trade Center Disaster: Experiments and Modeling of Multiple Workstations Burning in a Compartment, NIST Special Publication NCSTAR 1-5E. National Institute of Standards and Technology. Gaithersburg, MD, June 2005.
31. OMEGA Engineering Inc., Appendix B, Thermocouple Characteristics in The Temperature Handbook, 2000.
32. Mulholland, G.W., and Croakin, C., *Specific Extinction Coefficient of Flame Generated Smoke*, Fire and Materials, 24, 227-230, 2000.
33. Bryant, R., Womeldorf, C., Johnsson, R., and Ohlemiller, T., *Radiative heat flux measurement Uncertainty*, Fire and Materials, 27:209–222 (2003).
34. Pitts, W.M., Murthy, A.V., de Ris, J.L., Filtz, J.-R., Nygård, K., Smith, D., Wetterland, I., *Round Robin Study of Total Heat Flux Gauge Calibration at Fire Laboratories*, National Institute of Standards and Technology (NIST), Special Publication 1031, October 2004.
35. Walton, W.D. and Thomas, P.H., *Estimating Temperatures in Compartment Fires,* The SFPE Handbook of Fire Protection Engineering, 3rd Ed., (Section 3, Chap 6), National Fire Protection Association and The Society of Fire Protection Engineers, Quincy, MA, (Eds.: P. J. DiNenno, D. Drysdale, C. L. Beyler, and W. D. Walton), 2003.
36. Alpert, R.L., *Ceiling Jet Flows*, The SFPE Handbook of Fire Protection Engineering, 3rd Ed., (Section 2, Chapter 2), National Fire Protection Association and The Society of Fire Protection Engineers, Quincy, MA, (Eds.: P. J. DiNenno, D. Drysdale, C. L. Beyler, and W. D. Walton), 2003.
37. Milke, J.A., *Smoke Management in Covered Malls and Atria*, The SFPE Handbook of Fire Protection Engineering, 3rd Ed. (Section 4, Chapter 13), National Fire Protection Association and The Society of Fire Protection Engineers, Quincy, MA, (Eds.: P. J. DiNenno, D. Drysdale, C. L. Beyler, and W. D. Walton), 2003.
38. Heskestad, G., *Fire Plumes, Flame Height and Air Entrainment,* The SFPE Handbook of Fire Protection Engineering, 3rd Ed. (Section 2, Chap 1), National Fire Protection Association and The Society of Fire Protection Engineers, Quincy, MA, (Eds.: P. J. DiNenno, D. Drysdale, C. L. Beyler, and W. D. Walton, eds.), 2003.
39. Heskestad, G., *Luminous Heights of Turbulent-Diffusion Flames*, Fire Safety J. 5, 103-108 (1983).

A DOCUMENTATION OF PERSONAL COMMUNICATIONS

Bundy, Matthew, NIST, Gaitherburg, MD. Conversation at NIST during May, 2005 on determination of the combustion efficiency and the heat release rate in heptane spray flames in the NIST Large Fire Laboratory. Considering stoichiometry of the combustion and measurements in the exhaust hood, a combustion efficiency of 0.97 was determined for a 500 kW heptane spray fire.

Hostikka, Simo, VTT, Helsinki, Finland. Telephone conversation on May 2005 discussing the surface materials used during BE #2.

B TIME AVERAGING

Figure B-1 shows various periods used to time-average heat flux data acquired at 1 Hz for Gauge 9 during Test 13 of BE #3. The time response of the measurement itself is on the order of 1 s. The data used in this report were averaged over a 10 s period. Time averaging the data over too long a period may cause the loss of legitimate data and valuable information. No time-averaging at all, causes signal noise to play a role in the determination of peak values. This issue would have less significance if there had been many report experiments, and a statistically large number of peak values had been determined for one set of experimental conditions, but this was not the case. The selection of a 10 s averaging period is a compromise, but appears to be reasonable for the types of measurements considered in this report.

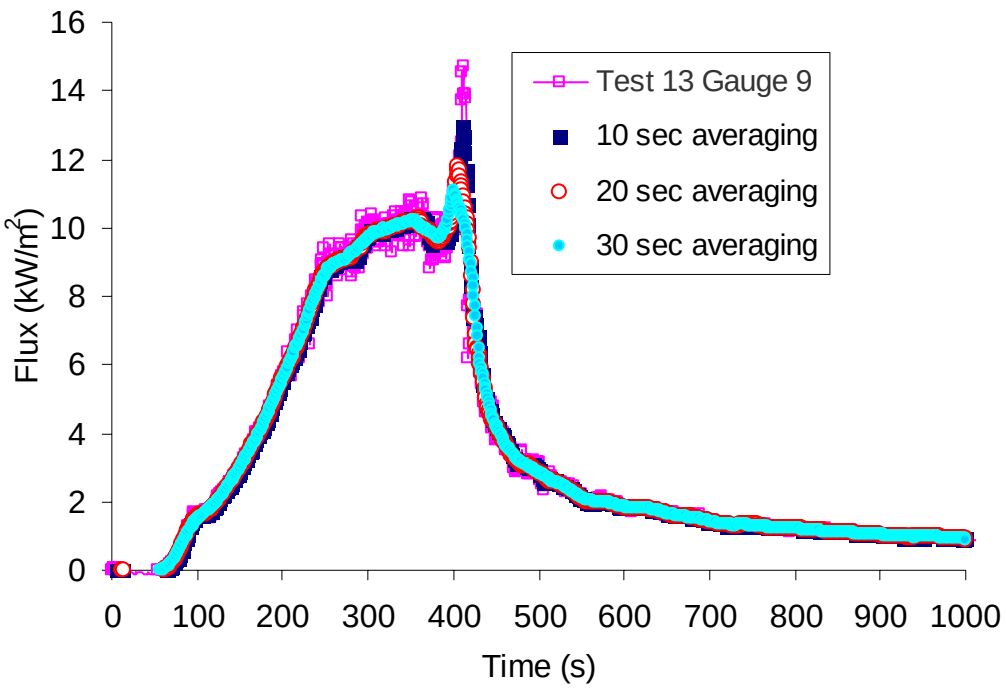

Figure B- 1: Various periods used to time average heat flux data acquired at 1 Hz for Gauge 9 during Test 13 of BE #3.